Journal Pre-proof

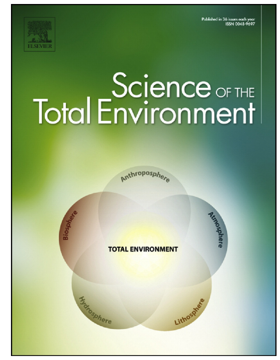

Land surface and air temperature dynamics: The role of urban form and seasonality

Marzie Naserikia, Melissa A. Hart, Negin Nazarian, Benjamin Bechtel, Mathew Lipson, Kerry A. Nice

PII: S0048-9697(23)05933-8

DOI: https://doi.org/10.1016/j.scitotenv.2023.167306

Reference: STOTEN 167306

To appear in: *Science of the Total Environment*

Received date: 20 July 2023

Revised date: 21 September 2023

Accepted date: 21 September 2023

Land surface and air temperature dynamics: The role of urban form and seasonality

Marzie Naserikia[1*], Melissa A. Hart[1], Negin Nazarian[1,2,3], Benjamin Bechtel[4], Mathew Lipson[5], Kerry A. Nice[6]

[1]Australian Research Council Centre of Excellence for Climate Extremes, University of New South Wales, Sydney, Australia
[2] School of Built Environment, University of New South Wales, Sydney, Australia
[3] City Futures Research Centre, University of New South Wales, Sydney, Australia
[4] Department of Geography, Ruhr-University Bochum, Bochum, Germany
[5] Bureau of Meteorology, Sydney, Australia
[6]Transport, Health, and Urban Design Research Lab, Faculty of Architecture, Building, and Planning, University of Melbourne, Melbourne, Australia

[*] email: m.naserikia@unsw.edu.au

Abstract

Due to the scarcity of air temperature (T_a) observations, urban heat studies often rely on satellite-derived Land Surface Temperature (LST) to characterise the near-surface thermal environment. However, there remains a lack of a quantitative understanding on how LST differs from T_a within urban areas and what are the controlling factors of their interaction. We use crowdsourced air temperature measurements in Sydney, Australia, combined with urban landscape data, Local Climate Zones (LCZ), high-resolution satellite imagery, and machine learning to explore the interplay of urban form and fabric on the interaction between T_a and LST. Results show that LST and T_a have distinct spatiotemporal characteristics, and their relationship differs by season, ecological infrastructure, and building morphology. We found greater seasonal variability in LST compared to T_a, along with more pronounced intra-urban spatial variability in LST, particularly in warmer seasons. We also observed a greater temperature difference between LST and T_a in the built environment compared to the natural LCZs, especially during warm days. Natural LCZs (areas with mostly dense and scattered trees) showed stronger LST-T_a relationships compared to built areas. In particular, we observe that built areas with higher building density (where the heat vulnerability is likely more pronounced) show insignificant or negative relationships between LST- T_a in summer. Our results also indicate that surface cover, distance from the ocean, and seasonality significantly influence the distribution of hot and cold spots for LST and T_a. The spatial distribution for T_a hot spots does not always overlap with LST. We find that relying solely on LST as a direct proxy for the urban thermal environment is inappropriate, particularly in densely built-up areas and during warm seasons. These findings provide new perspectives on the relationship between surface and canopy temperatures and how these relate to urban form and fabric.

Keywords: air temperature, land surface temperature, crowdsourcing, remote sensing, land use data, local climate zone, urban heat

1. Introduction

Urban heat is a significant contemporary challenge that is caused by the combined effect of urban development and global climate change. It poses a multifaceted threat, impacting not only human health, well-being, and performance but also the energy efficiency and economy of cities (Nazarian et al., 2022). Heat exposure leads to adverse heat-related illnesses and subsequent morbidity challenges, such as cardiorespiratory diseases and infection (Aflaki et al., 2017; Méndez-Lázaro et al., 2018; Tan et al., 2010), with direct consequences to mortality (Gosling et al., 2009). Elevated urban temperatures can also increase demands for cooling and air conditioning and consequently increase energy consumption, greenhouse gas emissions, and anthropogenic heat in cities (O'Malley et al., 2015; Radhi et al., 2015).

There has been substantial research investigating urban heat and assessing the effectiveness of heat mitigation strategies for different cities. Much of this research uses satellite-based Land Surface Temperature (LST) to assess urban heat through bird's-eye view surface temperatures. However, canopy urban heat, measured by air temperature (T_a), is more directly relevant for public health and citizen thermal comfort (Martilli et al., 2020). The use of LST data for heat mitigation analysis is motivated by the consistent, global observation of the land surface provided by satellites (Zhou et al., 2019), whereas T_a is recorded only at locations where meteorological stations are available. Since air temperature varies significantly (both temporally and spatially) in urban areas, adequate data is needed to examine extreme urban air temperature (Kloog et al., 2014). The limited number of sensors used for monitoring air temperature presents a shortcoming in providing sufficient spatial details for mitigating the adverse effects of urban heat (Baranka et al., 2016; Wang et al., 2017).

To address this limitation, many studies have estimated T_a using weather stations and satellite-based LST data in different cities (Benali et al., 2012; Ho et al., 2014; Yang et al., 2017). However, the sites where T_a is measured are often from pseudo-urban locations such as airport fields or large parks, where T_a is not representative of the neighbourhoods where people live. This is because traditional observing networks of national meteorological organisations are installed to observe synoptic or large-scale features and intentionally avoid urban effects (Schlünzen et al., 2023). World Meteorological Organization (WMO) guidelines state observing stations should be "well away from trees, buildings, walls or other obstructions" (WMO, 2021). This leaves few locations within urban areas that conform with WMO standards; hence these observation networks are typically sparse and do not capture the spatial variability of air temperature in heterogeneous cities. Thus, T_a investigated by many studies may not be an appropriate reference for assessing urban heat in a more complex urban area with varying surface cover and structure.

Surface cover affects the temperature by modifying the moisture content, albedo, and cooling/heating capacity of the land surface, whereas surface structure and morphology influence airflow, the transfer of heat, and the radiation balance (Stewart and Oke, 2012). To characterise this variability in cities and capture this intra-urban temperature variation, Stewart and Oke (2012) introduced the concept of a Local Climate Zone (LCZ). This classification method is used to distinguish microclimate variability based on urban neighborhoods and natural land cover.

A consensus on the interaction between LST and T_a has not yet been reached. Some studies stated that T_a and LST show similar patterns at night (Dousset, 1989). However, the relationship between LST and T_a during the daytime and across different urban landscapes remains elusive. Previous research presents conflicting results: studies in Shanghai and Hangzhou, China (Cai et al., 2018) and Sendai, Japan (Zhou et al., 2020) compared the distribution of LST and T_a across LCZs. The former found similar air and surface temperature patterns across all LCZs, whereas the latter observed a stronger relationship with LCZs for LST compared to T_a. A study in Shenzhen, China, assessed the intra-city spatial pattern of T_a and LST (derived from MODIS imagery) and observed that there was a positive relationship between these two temperatures, but they differed in the spatial patterns of hot and cold spots (Cao et al., 2021). Further, there have been studies comparing weather station T_a with satellite-based LST at regional and global scales (Jin and Dickinson, 2010; Zhang et al., 2014), stating that they are positively correlated, and their relationship depends on land cover type and other factors. However, numerous studies have suggested that canopy and surface urban heat islands may have different diurnal and seasonal patterns (Chakraborty et al., 2017; Ho et al., 2016; Krelaus et al., 2023; Venter et al., 2020; Venter et al., 2021; Wang et al., 2017).

This inconsistency among existing findings regarding the interaction between LST and T_a might be attributed to a limited number of weather stations with inadequate spatial coverage, which makes it difficult to capture intra-urban temperature variability in heterogeneous cities and may result in measurement biases. Thus, the question of how LST interacts with T_a in heterogeneous urban areas remains largely unaddressed due to a lack of in situ observations of T_a within many cities (Stewart et al., 2021). Such discrepancies also imply uncertainty regarding the application of remotely sensed LST to urban warming adaptation and mitigation. When inferring T_a from LST, any discrepancies between the two could potentially influence how adaptation/mitigation efforts that are intended to modify T_a are assessed using remote sensing. In addition, uncertainties exist concerning the surfaces being monitored through remote sensing (mostly roofs and top of the canopy). The particular viewing geometry of satellites could potentially limit the accuracy with which mitigation efforts are assessed, as they may not capture all relevant surfaces within an urban landscape.

In recent years, the “Internet of Things” (IoT) sensing has enabled urban data to be gathered from and by the public using citizen-science solutions that cover a wide range of temporal and spatial temperature distributions in cities (Middel et al., 2022; Potgieter et al., 2021). The data collected through citizen weather stations have been used to assess urban thermal climate in multiple cities (Chapman et al., 2017; Du et al., 2023; Fenner et al., 2017; Varentsov et al., 2020) but with a limited focus in coastal cities. This high-density crowdsourced temperature data, in combination with high-resolution satellite imagery and clear metadata on urban characteristics in cities, can provide the opportunity to understand how applicable satellite-based LST is in comparison with T_a. In other words, how does LST interact with T_a within the city, and what are the contributing factors to the variability of their relationship?

Here, we address these questions by focusing on Sydney, Australia, which has a complex nature due to its substantial geographical differences between inland and coastal areas. Studies have shown the occurrence of urban heat in Sydney (Hirsch et al., 2021; Livada et al., 2019; Ma et al., 2017; Sidiqui et al., 2016) is mostly exacerbated by urban development and local climate patterns. To reduce the adverse effects of urban heat and support the sustainability and resilience of urban districts that experience accelerated warming in this city, it is essential to characterise intra-urban heat and identify the key factors associated with urban warming from a micro to a city scale. However, exploring the thermal environment in this metropolitan area is challenging as it is a temperate coastal city affected by sea and Foehn-like breezes, and exposed to the effect of the Australian arid biome, one of the biggest desert areas worldwide (Yun et al., 2020). Western Sydney, which is closer to the Australian arid biome, experiences a more continental climate with a larger diurnal temperature range, while Eastern Sydney shows a more moderate, coastal climate with a lower diurnal temperature range. This geographical and climatic distinction between coastal and inland regions adds layers of complexity to the city's thermal environment. Hence, a comprehensive study is required to characterise urban heat in Sydney, which serves as a prime example of a region with a complex system that can be analysed to explore the dynamics of LST/T_a interactions.

In the current study, we leverage data from crowdsourced monitoring stations combined with LST derived from Landsat imagery and urban datasets (such as LCZs and building-level urban data) to quantify the spatial pattern of LST and T_a and their seasonal variability in Sydney. We aim to understand how LST and T_a interrelate during different seasons and further assess the potential of satellite-based LST for investigating heat mitigation strategies aimed at improving citizens' thermal comfort.

2. Data and Methods

2.1. Study area

The Sydney metropolitan area, which is located on the southeast coast of Australia (Fig. 1), has a temperate climate with mild winters and warm summers. The average annual temperature in Sydney is 17.8 °C, with 1200 mm of precipitation throughout the year, and elevation ranging from 0 to 500 m. It has a population of 5 million (Australian Bureau of Statistics, 2021). The city's rapidly expanding urban area has contributed to increasing the city's vulnerability to urban heat effects. Despite the importance of urban warming in Sydney, only a few studies have been conducted in this metropolitan area. Most of these studies have used fixed-point air temperature data from synoptic-scale meteorological forecasting networks (Sidiqui et al., 2016), whereas characterising surface temperature has been less explored. Thus, using a more appropriate air temperature dataset combined with remote sensing satellite imagery and clear metadata on urban characteristics may be a more suitable approach for monitoring surface and canopy urban heat, exploring the impact of urbanisation, and identifying the drivers of intra-urban variability across Sydney.

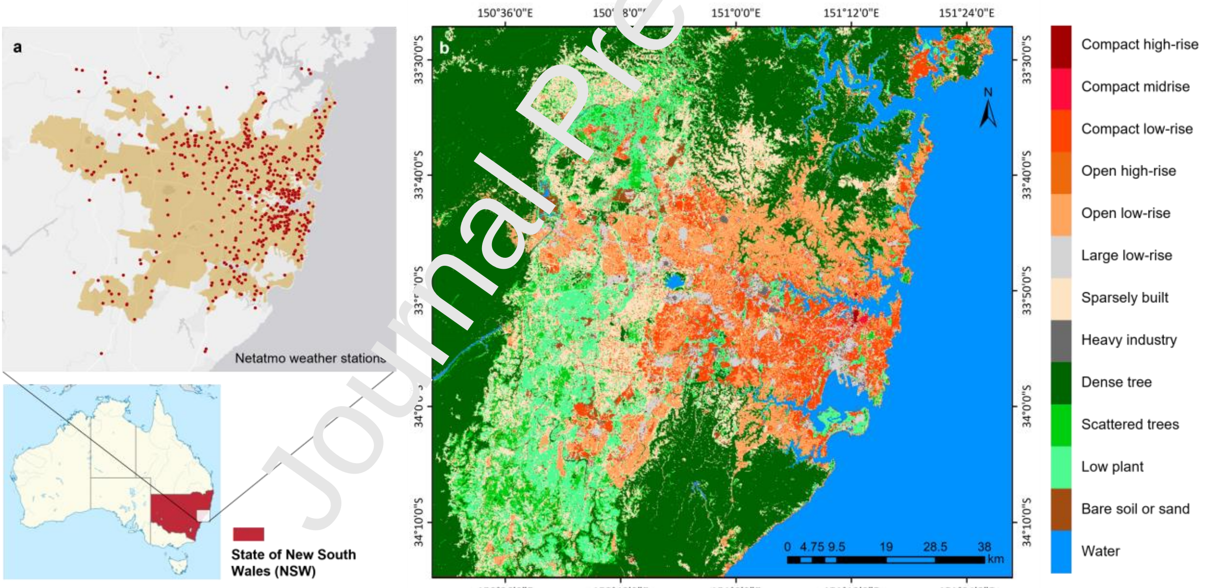

Fig. 1. The location of the study area. a) Netatmo weather stations over Sydney, Australia. b) Local Climate Zone (LCZ) map of Sydney.

2.2. Urban landscape data

In order to comprehensively explore urban land cover and structure in Sydney, we use an LCZ map, with a resolution of 100m, obtained from a global LCZ map created by Demuzere et al. (2022). This standardised landscape classification system enables a consistent comparison of various regions in urban areas. However, the absence of direct spatial or building height information in the satellite imagery used to generate the LCZ maps is a limitation of this urban dataset. To further understand the urban landscape, we also use the "Geoscape" dataset derived from building-resolving, 3D land cover data at 2m (Lipson et al., 2022). This open dataset enables the categorisation of building height and elevation along with impervious surfaces and vegetation, with a resolution of 300 m. The Geoscape variables used in this study include building and road path fraction, frontal density (the ratio of the frontal area and the total surface area used for analysing urban ventilation corridors), building height, low vegetation fraction (e.g. grass), tree fraction, water fraction, and sky view factor (referring to the fraction of visible sky when viewed from a surface and influences on the microclimate by trapping heat and providing shade in urban areas).

2.3. Satellite remote sensing data

For determining LST in Sydney, we selected sixteen Landsat 8 images captured on cloudless days during all seasons from 2019 to 2022 via the United States Geological Survey (USGS), Earth-explorer website (earthexplorer.usgs.gov). The Landsat imagery has a spatial resolution of 100 m and corresponds to 10 am (+/− 15 min) mean local time. LST maps were computed and extracted using Google Earth Engine (GEE), which is a geospatial cloud-computing platform (Gorelick et al., 2017). The Statistical Mono-Window (SMW) algorithm was used to calculate land surface temperature (LST) from Meteosat First and Second Generation satellites. The algorithm is developed by the Climate Monitoring Satellite Application Facility (Duguay-Tetzlaff et al., 2015) and uses an empirical relation between top-of-atmosphere brightness temperatures and LST in a single thermal infrared channel. It is based on a linearisation of the radiative transfer equation and takes into account surface emissivity from ASTER Global Emissivity Database with a correction for vegetation dynamics using NDVI. The LST maps retrieved from this algorithm have been demonstrated to achieve a satisfactory level of accuracy (Ermida et al., 2020).

$$LST = A_i * \mathrm{Tb}/\varepsilon + B_i * 1/\varepsilon + C_i \quad (1)$$

where T_b refers to the top-of-atmosphere brightness temperature in the thermal infrared channel and ε represents the surface emissivity of the channel. The coefficients A_i, B_i and C_i are calibrated for different classes based on the values of total column water vapour and view zenith angle.

2.4. Crowdsourced Weather station data

Crowdsourced air temperature data were collected from over 800 Netatmo citizen weather stations scattered throughout Sydney. Since historical crowdsourced data is not available, the data used in this study was obtained by recording Netatmo data for the 16 selected cloudless days from 2019 to 2022. Netatmo weather stations are composed of two modules, indoor and outdoor. The outdoor module used in this study measures real-time weather variables such as air temperature and humidity with accuracy of ±0.3°C and 3%, respectively. The collected outdoor data is then displayed on the Netatmo Weathermap web portal if the user consents to share the data (Fenner et al., 2021).

Sensors placed in shaded areas tend to provide accurate readings; however, those located in direct sunlight, indoors, or in other improper locations may produce inaccurate measurements (Varentsov et al., 2020). Therefore, a quality control process was applied to the dataset, filtering it according to the five main steps outlined in the framework developed by Fenner et al. (2021). This process removed temperature readings: (a) taken by stations with duplicate coordinates; (b) deemed outliers based on their z-score compared to other readings; (c) if more than one-fifth of the readings in a whole month were filtered out in the previous steps; (d) if the readings are determined to have been taken indoors due to a weak correlation with the median temperature of all readings; and (e) with unrealistically high values that were deemed outliers compared to the adjacent stations. To facilitate comparisons among stations following the QC process, T_a data were adjusted for elevation variations relative to a reference height. This reference height was determined as the average elevation of all professionally-operated weather stations within the city.

2.5. Statistical analysis

We conducted statistical analyses of the relationship between T_a and LST across different seasons and locations in Sydney. For this purpose, we retrieved the LST values of the pixels where the weather stations were located and used them as the surface temperature corresponding to those stations on each selected day. We first compared the range of LST and T_a for all the stations during different seasons in Sydney. Days are arranged in chronological order based on months and days, but not years, except for summer. We have also considered daily minimum and maximum air temperatures obtained from the Australian Bureau of Meteorology website (bom.gov.au). Each day was assigned to a season based on how well that aligned with climatological mean conditions for that season. Since the meteorological conditions of Sep 2020 closely resembled those of summer days, the analysis for this day was shifted into the summer season.

A seasonal comparison of LST and T_a variability across the primary Sydney LCZs, and their temperature differences and spatial variability were mapped for the individual days within the study area. In this analysis, we focused on the main LCZs in Sydney: 3. compact low-rise, 6. open low-rise, and 8. large low-rise, 9. sparsely built, and A. dense trees and B. scattered trees. These are also the categories with the highest number of Netatmo stations.

We analysed the spatial autocorrelation of LST and T_a to identify the spatial clusters of high and low-temperature values across different seasons in Sydney. We used the Hot Spot Analysis (Getis-Ord Gi*) tool in ArcMap 10.8, which enables identifying statistically significant spatial clusters of hot and cool spots. The Getis-Ord Gi* statistical value and p-value can be calculated by this tool for each feature in the dataset. While a feature with a high value may be interesting, it doesn't necessarily indicate a statistically significant hot spot. To be considered a statistically significant hotspot, a feature must have a high value and be surrounded by other high-value features (Getis and Ord, 2010). We also conducted Pearson correlation analysis to investigate LST-T_a relationships as well as the effects of Geoscape variables (such as building height, tree fraction, water fraction, etc.) on LST and T_a across the primary LCZs in Sydney during different seasons.

Moreover, we employed machine learning methods to comprehensively investigate the impact of urban form and fabric on LST variability across different seasons in Sydney. Specifically, we used the Gradient Boosting (GB) regression technique which combines decision trees in sequence. At each step, a new tree is generated based on the prior performance, resulting in a robust model that minimises prediction errors (Friedman, 2001). With this machine learning approach, we were able to determine the contribution of urban morphology (Geoscape and terrain variables) on LST variation as the target variable. For all the analyses, 70% of the data was used for model training, while the remaining 30% was reserved for testing the performance of the model after training. The trained model performance was measured using adjusted R^2 and RMSE, and to minimise the effect of random sampling (test and train splitting), we performed the entire process ten times.

Feature importance in a GB model is a metric that indicates how much each variable contributes to the reduction of the model fit variance. To examine the effects of urban form and fabric on LST, we determined the importance of individual explanatory features for each selected day. It is worth noting that we minimised the effect of potential multicollinearity before calculating the feature importance as collinearity can distort model estimation when the correlation coefficients between explanatory variables exceed a threshold of 0.7 (Dormann et al., 2013; Naserikia et al., 2022). For each day, we trained the GB model with different permutations of n variables, where n was chosen to maximise the number of predictors for model training, while satisfying the collinearity threshold (R = 0.7). We then calculated the variables' importance only if the corresponding model achieved an acceptable prediction performance on the test dataset ($R \geq 0.8$). To enhance the robustness of the results, we repeated the entire process five times using different random portions of the data as the test and train sets. Lastly, we calculated the average importance scores and presented them in bar charts for each individual day. The framework of the study is presented in Fig. 2.

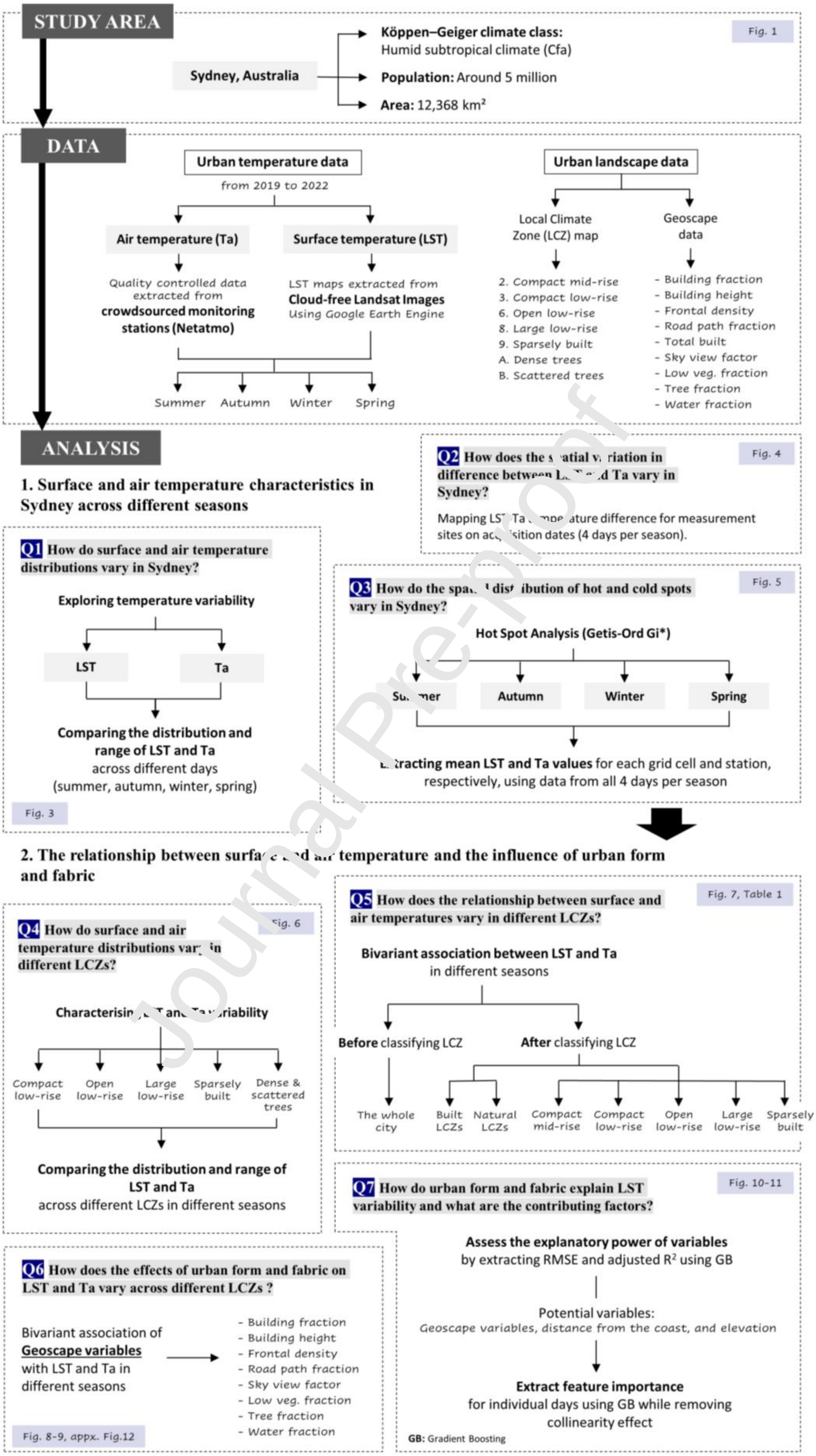

Fig. 2. The research framework of the study

3. Results and Discussion

3.1. Surface and air temperature characteristics in Sydney across different seasons

In this section, we use crowdsourced weather station data in Sydney, Australia, combined with remote sensing satellite images to explore surface and air temperature characteristics and the intra-urban temperature variabilities during different seasons.

3.1.1. Variability of LST and T_a values

To understand how LST and T_a differ in Sydney, their spatial and temporal variability is investigated across different seasons. Fig. 3 shows that there is greater seasonal variability in LST compared to T_a. The largest inter-seasonal variation in urban temperature can be observed during the transitional seasons (autumn and spring), while the lowest is seen in winter when temperatures tend to be more stable and consistent throughout the city. Except for winter, LST was found to have consistently higher values than T_a on the selected days. A significantly higher maximum LST can be seen in summer observations (ranging from 46.8 to 57.3 °C) compared to other seasons. This can be attributed to several factors, including sun angle, the intensity of solar radiation, and longer days. During summer, solar insolation is greater contributing to the significantly higher maximum LST values observed on warm days.

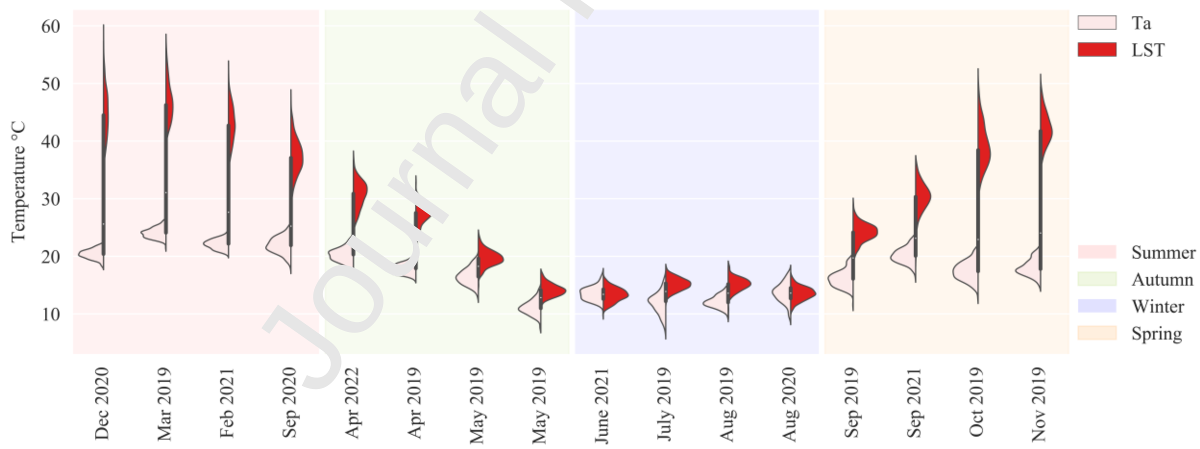

Fig. 3. Range and distribution of LST and T_a values for Sydney across different days (summer, autumn, winter, and spring, respectively). Coloured areas of the violin plots represent the distribution of LST and T_a values. Days are arranged in chronological order based on months and days, but not years, except for summer. Each day was assigned to a season based on its alignment with climatological mean conditions for that season. Since the meteorological conditions of Sep 2020 closely resembled those of summer days, the analysis for this day was shifted into the summer season. Within the summer season, the days were sorted based on maximum LST values.

LST values show larger ranges in summer (24.3 - 57.3 °C) and spring (18.2 - 49.9 °C) than in autumn (11.3 - 36.7 °C) and winter (9.5 - 18.3 °C). During winter, LST values are highly concentrated around the median (ranging from 13.3 to 15.2 °C), while during summer, they are more dispersed and show a more elongated distribution. This indicates that LST varies greatly within the city from October to February (late spring and summer), with values differing considerably from T_a during this period.

However, from April to October (autumn, winter, and early spring), there is no significant difference in the intra-urban variation of LST and T_a. The greater ranges of LST in summer likely result from the earlier sunrise and higher sunshine intensity leading to greater warming on sunlit surfaces compared with other periods. With the satellite temperature observations taken in the mid-morning, at approximately 10 am, most shaded surfaces will have not yet been exposed to sunlight since cooling overnight.

The significant seasonal variability in LST spatial heterogeneity found in this study is consistent with results from seasonal LST assessment in global cities with varying background climates (Naserikia et al., 2022). However, our findings contrast with previous research conducted in Shenzhen, China (Cao et al., 2021). Despite Shenzhen's climate similarities to Sydney, this study found no significant difference in LST between different seasons during the day. The discrepancy in findings may be attributed to the satellite data used for extracting LST in these studies. The study of Shenzhen employed MODIS data, which has a coarser resolution compared to the Landsat imagery used in this research. In addition, Shenzhen, located at ~22°N, experiences a less pronounced seasonal variation compared to Sydney's ~33°S latitude, resulting in a generally more seasonal climate in Sydney. Additionally, the summer months in Shenzhen have more cloud cover, which is supported by the average monthly hours of sunshine being around 200 hrs/month in Shenzhen compared to approximately 250 hrs/month in Sydney. A moister climate would likely reduce the range of LST (from soil moisture/vegetation). The exact timing of satellite flyover could also play a role, as different timing can influence LST measurements. Furthermore, pollution, which can be considerable in Shenzhen due to emissions in the Pearl River Delta conglomerate of cities with a high population density (85 million), might contribute to the lower LST variability observed in summer.

Fig. 3 also shows that the ranges of LST and T_a values are very similar in all winter days and most autumn days, while there is a significant difference between the range of these two temperature variables in summer and spring. This pattern is mainly attributed to the variation in solar radiation. During winter, the strength of the solar radiation is lower than it is in summer, and for LST, solar radiation is a dominant factor, especially at the time of capturing temperature data (10 am). In contrast, for T_a, there are materials in the urban environment that absorb heat and release it later, resulting in a delayed effect of solar radiation on air temperature during summer. Therefore, we do not see an immediate effect of solar radiation on T_a. Furthermore, for LST, the larger zenith angle during winter at the same satellite overpass time leads to increased shadowing, further influencing surface temperature readings. For T_a, winter conditions often present increased levels of moisture. This tends to reduce overnight cooling, which in turn narrows the daily temperature range as well as altering the energy balance to reduce sensible heat flux and more effective conduction of heat away from the surface.

3.1.2. Spatial variations in temperature difference between LST and T_a

To better understand how T_a differs from LST across Sydney, we calculated the difference between the two at all T_a measurement sites. As shown in Fig. 4, the temperature difference between LST and T_a varies across the seasons. During summer, the temperature difference (LST - T_a) can vary widely, ranging from 9 to 38 °C. In contrast, during winter, the range of difference is smaller, with values ranging from -7 to 9 °C. In autumn, the difference ranges from -2 to 17 °C, whereas in spring, it ranges from 2 to 33 °C. Studies examining surface and canopy urban heat have found that LST is usually higher than T_a during the daytime (Hu et al., 2019; Shreevastava et al., 2021), which we see for the most part in Sydney; however, we also observe equal or lower LST than T_a in some measurement sites during cold days, resulting in a negative difference ($-7 < LST - T_a < 0$). This may be due to the reduced solar radiation, which results in less energy being absorbed by urban surfaces. In addition, variations in surface thermal properties and/or warmer air being advected into the area can contribute to lower LST values compared to T_a during the cold months.

The largest temperature difference is observed during summer and late spring, whereas the smallest difference can be seen during winter. The spatial variability in LST-T_a difference within the city is also largest during summer and spring, while the lowest is observed during the winter days. This difference tends to increase with increasing distance from the coast, particularly during warm days (Fig. 4), highlighting the moderating influence of the ocean on T_a. Fig. 3 also indicates that less built-up areas tend to show a smaller difference between LST and T_a. In particular, the stations located in the northern coastal part of the city tend to exhibit a smaller temperature difference compared to those in denser built-up areas such as the central and western parts of the city. This illustrates the role of urban complexity, specifically the interplay between geography and urban form and fabric, in shaping temperature patterns. A recent study has also demonstrated the notable impact of this complexity on air temperature distribution across Sydney (Potgieter et al., 2021).

In built-up areas, there is a higher proportion of impervious surfaces (such as pavements, roads, and buildings) that absorb and store heat more readily compared to natural surfaces. These areas also have a lower albedo and absorb more solar radiation, leading to an increase in surface temperatures and wider differences between LST and T_a. Some parts of the urban surfaces such as well insulated roofs do not efficiently store or conduct heat. When dry, they can rapidly heat up under direct solar radiation exposure, thereby broadening the LST distribution at the time of Landsat satellite overpass. In contrast, natural areas have a higher albedo and are more porous, allowing for greater storage of water, which can regulate temperatures through evaporation. Additionally, the presence of vegetation provides shade and cooling through transpiration, further reducing LST and narrowing the difference between LST and T_a in less built-up areas.

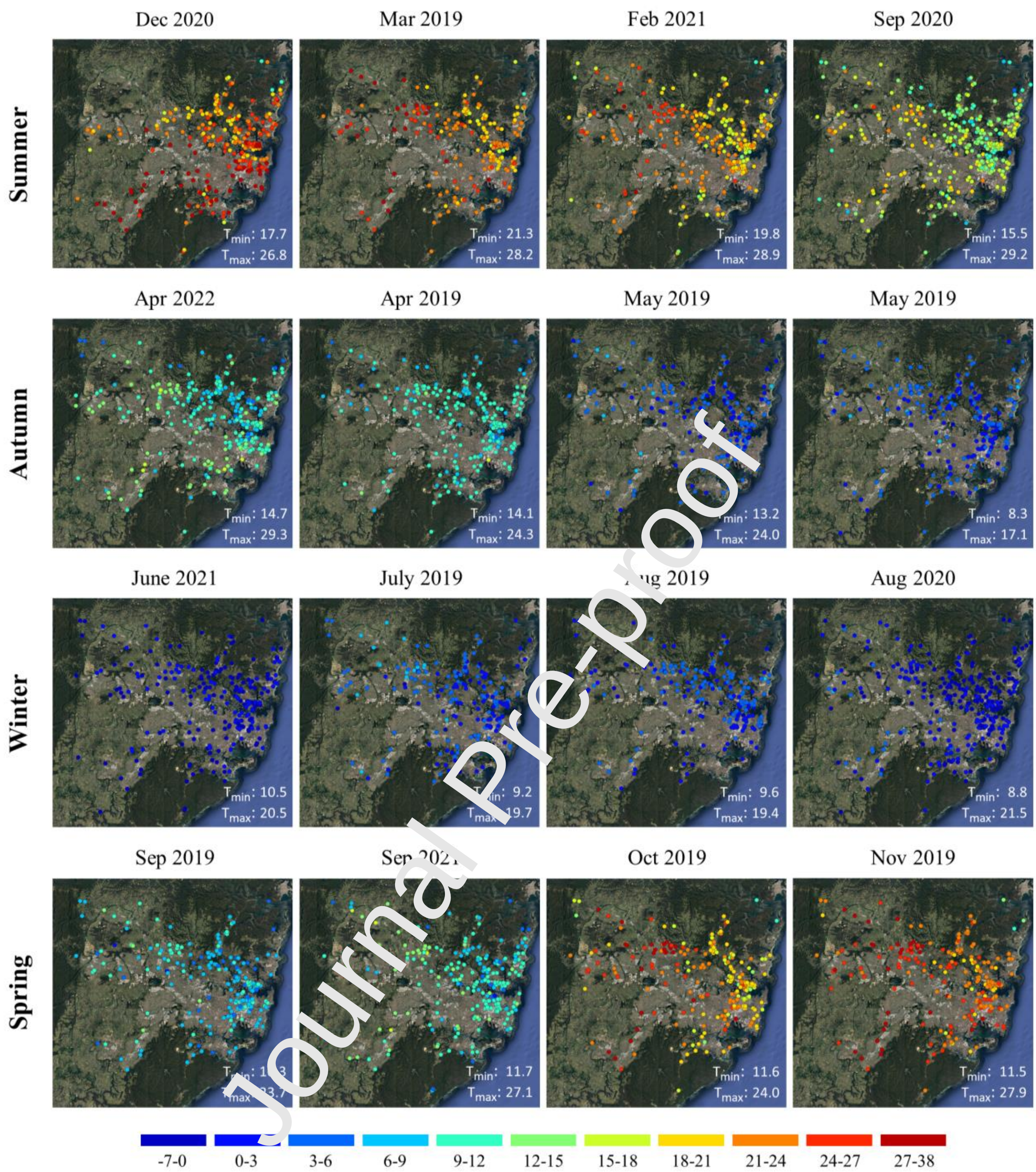

Fig. 4. The temperature difference between LST and T_a on acquisition dates in Netatmo stations across Sydney. The daily min and max air temperatures (°C) - obtained from Australian Bureau of Meteorology (BoM) - are shown in the bottom right corner of each map. Each day was assigned to a season based on its alignment with climatological mean conditions for that season.

3.1.3. Spatial distribution of LST and T_a hot and cold spots

To gain a better understanding of the distribution of hot and cold spots for LST and T_a in Sydney during different seasons, we conducted a spatial analysis using Hot Spot Analysis (Getis-Ord Gi*). Our findings, illustrated in Fig. 5, demonstrate significant seasonal variability in the occurrence of LST hot and cold spots. During summer and spring, LST hot spots are predominantly located further inland, away from the coast. This is not only because the central parts of the city generate and trap more heat but also due to the cooling effect of sea breezes along the coast, which limits the extent of LST hot spots. In contrast, the higher heat capacity of the ocean enables it to act as a heat source in winter, keeping coastal areas warmer than inland. However, in the western and central parts of the city, the moderating influence from the ocean is less impactful, which can result in cooler temperatures compared to coastal areas.

The distribution of cool and hot spots for T_a in Sydney differs from that of LST, and their respective cluster areas do not always overlap. However, a better match between LST and T_a hot spots can be seen in winter, with both observed in the coastal areas in the east. Previous research has demonstrated the significant influence of the distance from the ocean on air temperature, not only in Sydney (Potgieter et al., 2021) but also in other coastal cities such as Los Angeles (Vahmani and Ban-Weiss, 2016). However, for the distribution of T_a cold spots, our results show that vegetation plays an important role, this can be seen in the northern, inland regions of the city, which have greater vegetation cover compared to the coastal areas. Interestingly, the spatial pattern of cool and hot spots for T_a is more consistent across seasons than that of LST, indicating a relatively stable distribution of air temperature in Sydney throughout the year. The north, west, and south parts of Sydney are mostly situated in the non-significant and cold spot categories due to their proximity to mountains. The insights gained from these findings can assist decision-makers in identifying high-priority areas, optimizing urban vegetation, and allocating resources more effectively at the local scale.

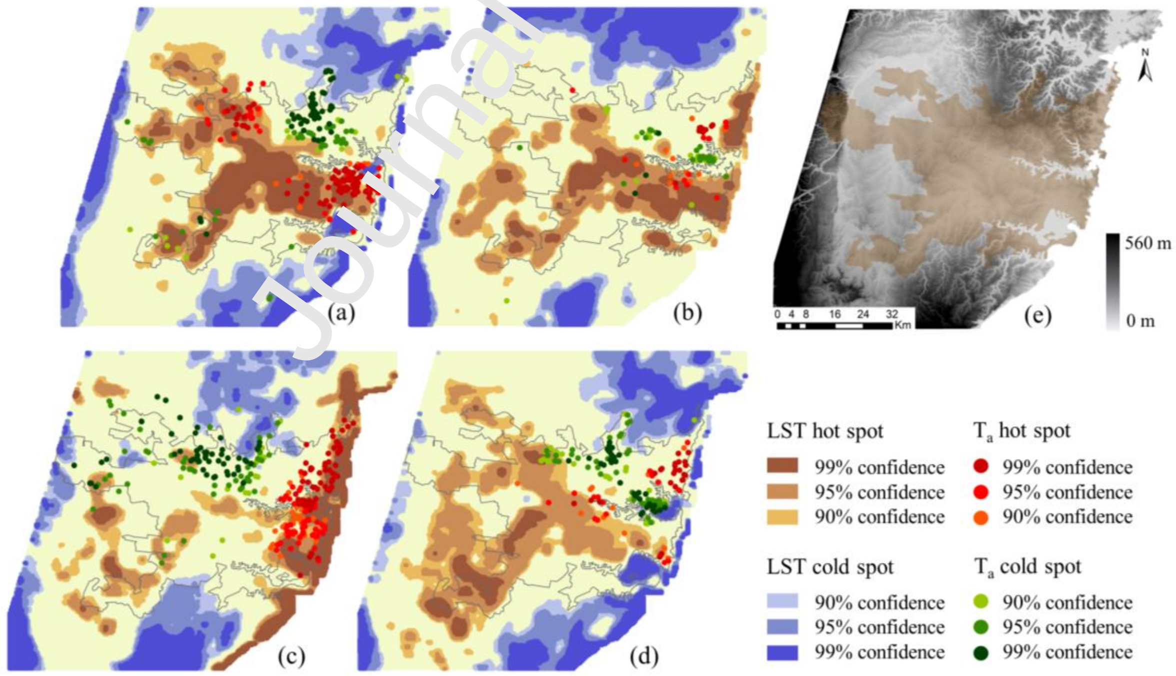

Fig. 5. Spatial distribution of LST and T_a hot and cold spots in Sydney across different seasons (a. summer, b. autumn, c. winter, and d. spring). e. shows elevation (grayscale) and city border (shaded brown) in the study area. The mean values of LST and T_a have been calculated for each grid cell and Netatmo station, respectively, using data from all four days in each season. Netatmo stations that were not classified as hot or cold spots were excluded.

3.2. The relationship between surface and air temperature and the influence of land cover and urban morphology

Previous studies have acknowledged that land cover and building characteristics play a significant role in shaping urban thermal environments (Krayenhoff et al., 2021; Masson et al., 2020; Nice et al., 2022). However, these studies have not analysed the individual contributions of these characteristics to LST and T_a and their relationship. To address this shortcoming, we used LCZ, surface cover, and building height data to explore the impact of urban form and fabric on intra-urban surface and air temperature variability in Sydney.

3.2.1. Seasonal variability of LST and T_a across different LCZs

Here, we assessed how LST and T_a distributions vary under different LCZs during different seasons in Sydney. Fig. 6 illustrates the boxplot distribution of LST and T_a in each day categorized by LCZ. Similar to Fig. 3, Fig. 6 shows that LST is generally higher than T_a in almost all days, with the largest difference in summer, and the lowest in winter. There is also a greater seasonal variation in LST compared to T_a. It also shows that the temperature difference between LST and T_a is higher in the built LCZs - particularly those classified as compact low-rise and large low-rise - compared to the natural ones. While the T_a values remain relatively consistent across various LCZs, the corresponding LST ranges show slight variations in these LCZs due to variability in surface cover, vegetation, and other physical characteristics. The LCZs with dense and scattered trees, low plants, soil, and sand tend to show the lowest LST values, followed by sparsely built areas, whereas compact low-rise and large low-rise show a higher LST range. The range of LST values observed in large low rise LCZs is similar to that of compact low-rise but higher than that of open low-rise LCZs, reflecting differences in the amount and type of surface cover and the associated heat storage and release. The higher LST values observed in large low-rise LCZs compared to open low-rise LCZs can be attributed to the presence of slightly more impervious surfaces and fewer green spaces in large low-rise LCZs, which leads to greater heat absorption and reduced evaporative cooling. These findings emphasize the importance of taking into account the specific characteristics of each LCZ in urban heat studies, especially when predicting T_a based on satellite-derived LST.

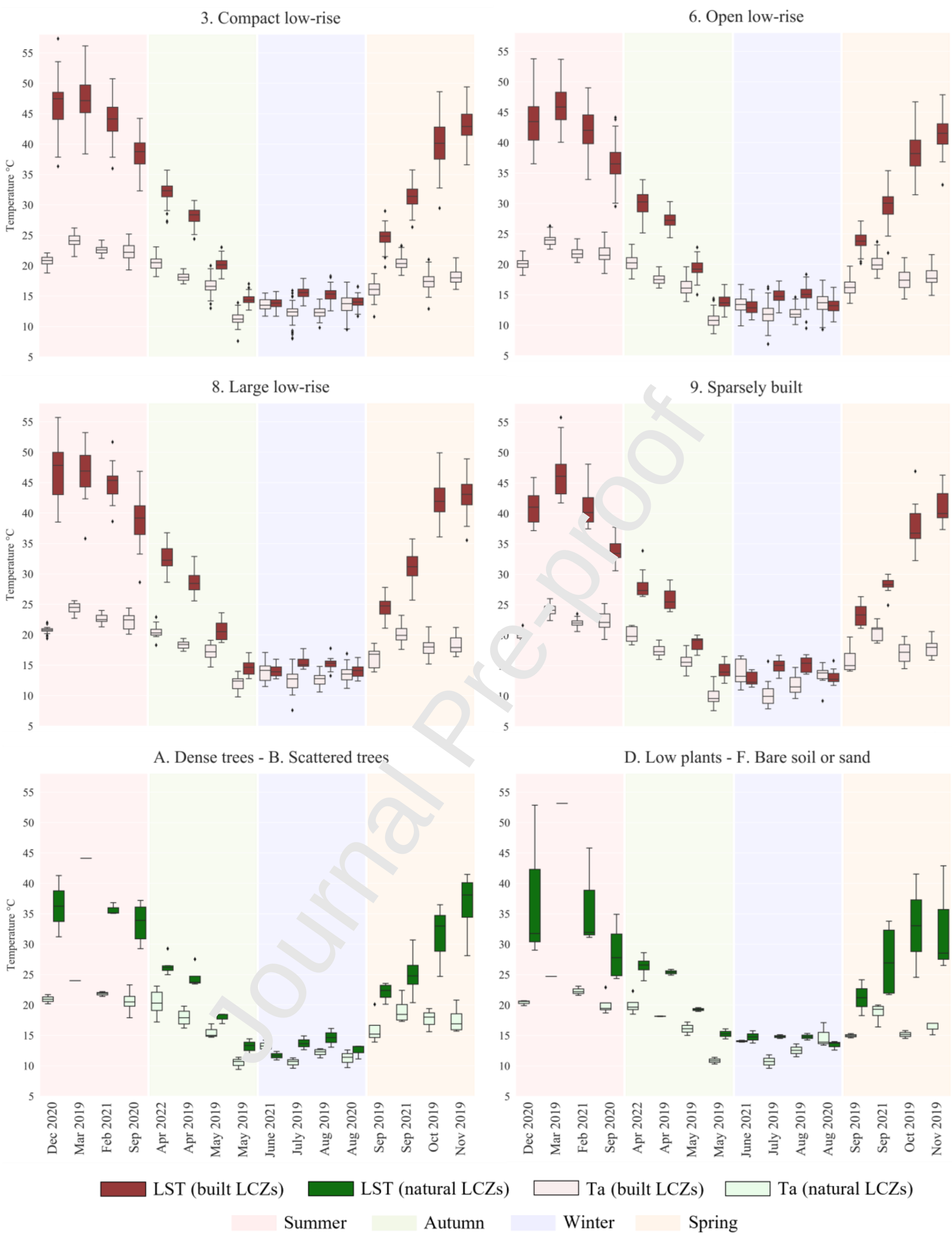

Fig. 6. Range and distribution of LST and T_a values across different days and seasons for the main LCZs in Sydney with the highest number of Netatmo stations. Days are arranged in chronological order based on months and days, but not years, except for summer. Each day was assigned to a season based on its alignment with climatological mean conditions for that season. Since the meteorological conditions of Sep 2020 closely resembled those of summer days, the analysis for this day was shifted into the summer season. Within the summer season, the days were sorted based on maximum LST values in all LCZs.

3.2.2. LST- T_a relationships across different LCZs

To investigate the relationship between LST and T_a, we conducted a Pearson correlation analysis. This allowed us to better understand how changes in surface temperature may influence the air temperature. Similar to previous research (Cao et al., 2021; Kim et al., 2021; Shen et al., 2020), we found a positive correlation between LST and T_a in all selected days. However, the proportion of variation in T_a explained by LST varies in different seasons. For instance, in summer, there are many data points with similar values of T_a, but their LST values differ considerably. The opposite was observed in winter days. This shows the complexity of the interplay between surface and air temperature in urban areas, which varies depending on the time of year.

As shown in Fig. 7, the Pearson correlation coefficient is slightly stronger in summer (ranging from 0.22 to 0.45) than that in other seasons (autumn: ranging from 0.15 to 0.37, winter: 0.08 to 0.35, spring: 0.17 to 0.35). This is in contrast with the findings of a study in Milton, Canada (Burnett and Chen, 2021), but consistent with another study in the Basin and Range province of the western United States (Mutiibwa et al., 2015). When combining all days in each season, the correlation is stronger in autumn (0.89) and weaker in winter (-0.11), indicating the highest inter-seasonal variations in T_a and LST values in autumn and the lowest in winter. These findings highlight the importance of seasonal variation in the LST-T_a relationship; however, they also confirm that the correlation between LST and T_a is affected by other factors beyond just seasonal changes, adding complexity to this relationship.

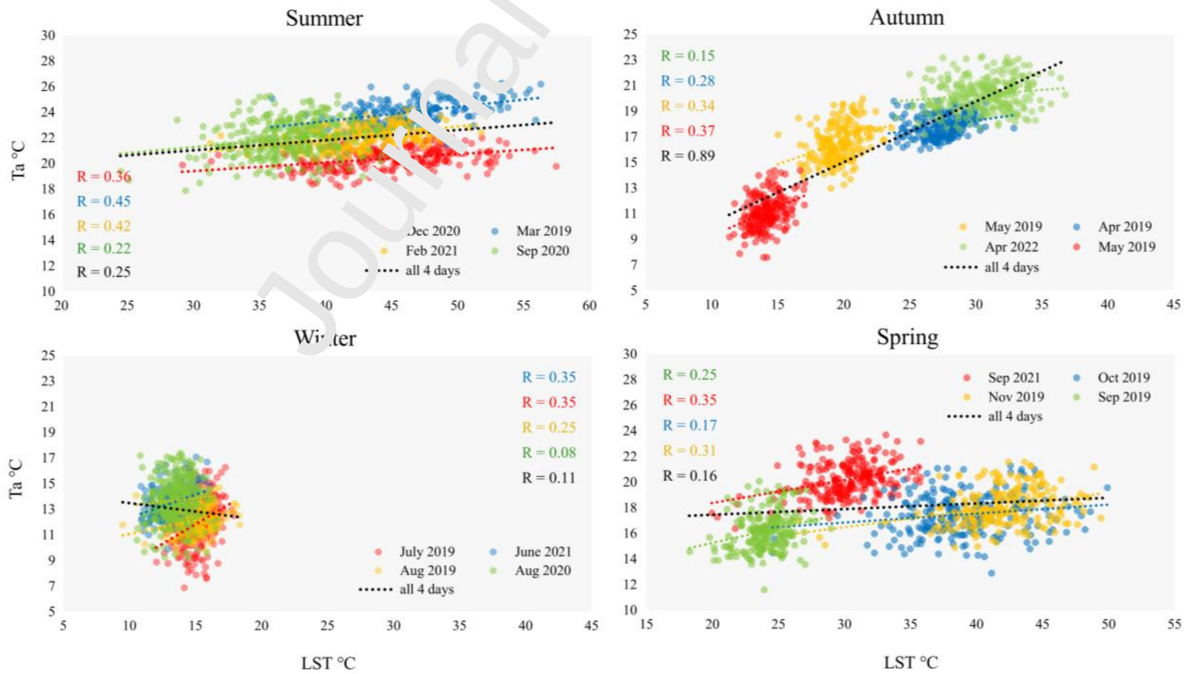

Fig. 7. The correlations between LST and T_a for Sydney across different days and seasons. All the relations are statistically significant at 0.05 level (except Aug 2020 with P-value of 0.18). Each day was assigned to a season based on its alignment with climatological mean conditions for that season.

To gain a deeper understanding of these factors and their impact, we conducted an analysis of LST-T_a correlations across different LCZs to investigate the role of surface cover and structure variability. In all LCZs (except for compact mid-rise), LST showed positive correlations with T_a (Table 1). Categorizing the stations based on the LCZs they are situated within results in a stronger relationship between LST and T_a. Interestingly, LST-T_a correlations tend to be stronger in less densely built-up areas. As indicated by Table 1, natural LCZs show a stronger relationship compared to built LCZs. A similar result was observed in a study conducted in southeastern China (Sheng et al., 2017), finding that this relationship was stronger in vegetated areas compared to impervious surfaces. Among the built LCZs, sparsely built and large low-rise LCZs mostly illustrate stronger correlations than open low rise and compact low rise. The closer correspondence between LST and T_a in less densely built-up areas may be attributed to the heat exchange between the land surface and the atmosphere, which is more direct and less influenced by human-made structures in natural LCZs and less built-up surfaces. Further, within the more dense built-up areas the sensor would be capturing mostly rooftops for LST, whereas T_a measurements would be from within the street canyon. Despite the limited data available for the compact mid-rise LCZ, strong negative correlations between LST and T_a were observed in this LCZ on two days (R > 0.8). This indicates that T_a decreases with increasing LST values in these regions, which could be attributed to shading caused by deeper building canyons (Johansson and Emmanuel, 2006; Masson et al., 2020), highlighting the importance of shading in moderating thermal environments in high-density urban areas.

This table can also show the importance of seasonal variability in the interplay between LST and T_a. Although the correlations may not be strong on individual days (~R < 0.4), considering the entire dataset for the entire year reveals a robust relationship (~R > 0.8) between LST and T_a across all LCZs, which is more climatological (rather than providing the ability to determine spatial variations of T_a from LST). However, the strength of the correlation varies significantly when accounting for season and urban form. These findings highlight that using LST as a direct proxy to represent urban air temperature and improve thermal environment may not always be appropriate, particularly when focusing on spatial patterns; however, they may provide insights for developing predictive models of air temperature using remotely sensed data when other key factors are taken into account.

Table 1: Correlation coefficient between LST and T_a across different LCZs.

Season	Date	Compact mid-rise	Compact low-rise	Open low-rise	Large low-rise	Sparsely built	Built LCZs	Natural LCZs	All LCZs
Summer	Dec 2020	×	×	0.29	0.43	0.63	0.38	×	0.36
	Mar 2019	×	0.44	0.56	×	×	0.45	×	0.45
	Feb 2021	×	×	0.55	×	×	0.42	0.8	0.41
	Sep 2020	×	×	0.15	×	×	0.15	0.56	0.22
Autumn	Apr 2022	×	×	0.14	×	×	0.16	0.55	0.15
	Apr 2019	×	0.24	0.26	×	0.45	0.32	×	0.28
	May 2019	×	0.41	0.28	×	×	0.33	×	0.34
	May 2019	0.85*	×	0.44	×	0.68	0.36	0.84	0.37
Winter	June 2021	×	0.21	0.49	×	×	0.35	×	0.35
	July 2019	×	0.39	0.4	×	×	0.35	×	0.35
	Aug 2019	×	0.2	0.19	×	0.68	0.25	×	0.25
	Aug 2020	×	×	0.16	×	×	×	0.74	0.08
Spring	Sep 2019	×	×	0.4	×	×	0.23	×	0.25
	Sep 2021	0.8*	×	0.39	0.69	×	[illegible]	0.76	0.35
	Oct 2019	×	×	0.21	0.39	×	0.14	×	0.17
	Nov 2019	×	0.18	0.2	0.44	×	0.25	0.61	0.31
All seasons	All days	0.85	0.85	0.84	0.83	0.81	0.84	0.78	0.83

× non-significant correlation or lack of data
* negative correlation

3.2.3. Impact of ecological infrastructure and building morphology on LST and T_a across different LCZs

Here, we extend the analyses to investigate the impact of surface cover determined by impervious and vegetated covers by exploring the correlation of urban morphology variables with LST (Fig. 8-Fig. ***9***) and T_a (Appendix A, Fig. A. 1) across different LCZs in Sydney. Fig. 8 shows the scatterplots for a single selected day presented as a sample, while Fig. 9 and Fig. A. 1 cover the entire study period and display the Pearson correlation coefficient values for all days included in this study. On almost all days, LST was found to be positively correlated with building fraction, frontal density, and road path fraction while showing negative correlations with sky view factor, building height, tree fraction, and water fraction. This illustrates the warming effect of building and road density on land surface, and the cooling impact of shading, open spaces, trees, and water. The strength of the relationship between these variables (except low vegetation and water fraction) and LST is generally higher in open low-rise LCZ and lower in large low-rise.

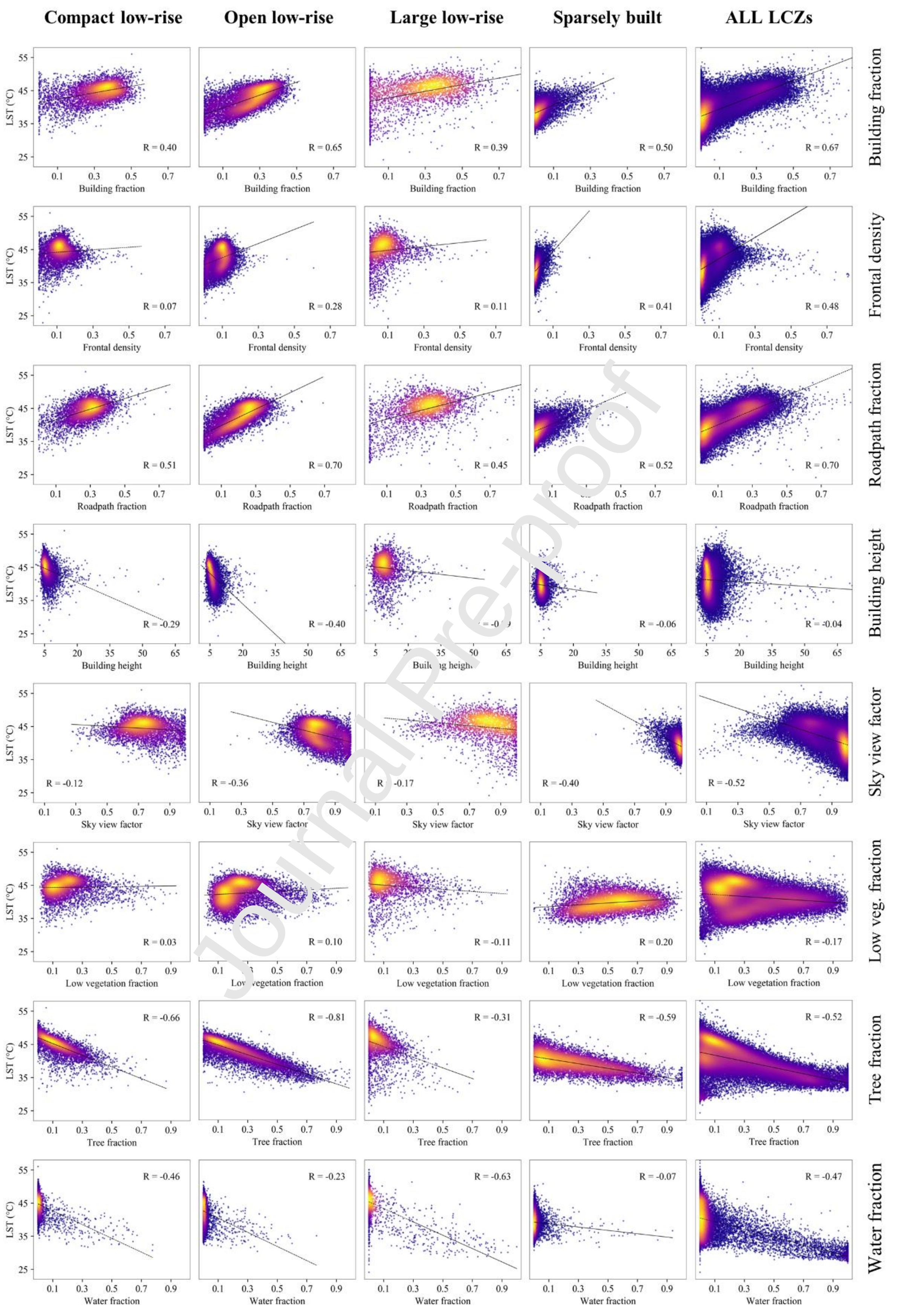

Fig. 8. A sample of the scatterplots showing the correlation between Geoscape variables and LST across different LCZs in Sydney on a summer day (Feb 2021).

Furthermore, a clear seasonal variation can be seen in the correlation between LST and urban morphology variables. The significance of the seasonal cycle was also observed in a study conducted in mainland China, showing a stronger relationship between LST and urban impervious surfaces in summer than in winter (Ma et al., 2016). As shown in Fig. 9, the strongest correlation between LST and building and road path fraction was observed from December to April (between 0.2 and 0.8). The strength of the correlation then decreases for winter days (from -0.2 to 0.4). However, in late winter, the correlation gradually begins to increase and continues to rise during the spring season. Although the built surfaces and roads remained largely unchanged across seasons, the increase in sunshine duration and intensity during warm months had an impact on surface temperature. The pattern of correlations between frontal density and LST is very similar to the previous two variables in all seasons except spring; like in winter, there is a less pronounced correlation between frontal density and LST across different LCZs during spring. However, on warm days, the greater impact of frontal density on LST highlights the significant role of wind-driven ventilation in regulating surface temperature (Yang et al., 2019). A recent study conducted in The Pearl River Delta in China has also demonstrated the notable impact of urban airflow on T_a, resulting from decreased frontal area density (Liu et al., 2021).

The effect of the sky view on LST shows a very similar pattern to frontal density but with opposite directions of correlation. The negative correlation between SVF and LST can be explained by the fact that in urban areas with higher SVF, the increase in built surfaces and higher roof fraction results in higher temperatures (Jamei et al., 2016). Urban areas with high SVF allow for more efficient cooling of the surface, whereas areas with low SVF can trap heat, lower ventilation performance, and increase temperature due to having less open sky and more obstructions (Yang et al., 2013). A recent study has also shown that a low SVF, resulting in reduced ventilation capacity, can contribute to elevated surface temperature during the day (Kim et al., 2022). Considering these, creating ventilation paths and open spaces in urban areas can be an effective mitigation strategy for surface and air urban heat as it can increase the sky view factor and decrease the density of the frontal area, thereby allowing for the movement of cooler air into urban areas and the removal of hot air. This can be achieved through the creation of open spaces, pedestrian walkways, squares, and plazas in built-up areas. However, the effectiveness of these approaches may depend on their connectivity to areas of cooler air to enable efficient advection. It is important to consider local climate conditions; for instance, increased sky view factors could lead to reduced shading and greater exposure to solar radiation, which may not be beneficial in hotter and drier climates.

Building height and spacing has often been found to be the main factors influencing urban climate (Cai et al., 2018; Mou et al., 2017; Nice et al., 2022). Whereas, studies investigating the relationship between building height and LST have reported conflicting results, with some suggesting a positive correlation between building height and LST (Guo et al., 2016), while others have found negative relationships, which means taller buildings are associated with lower LST (Zheng et al., 2019). This inconsistency among different findings may be attributed to the variation in the urban landscapes of the study areas, such as differences in the percentage of vegetation and impervious surfaces, as well as differences in the background climates. Moreover, the relationship between building height and LST is not solely dependent on height, but it is influenced by both height and density of buildings. When buildings are densely packed, the influence of building height on LST is limited because the shadows cast by taller buildings are not clearly visible. The timing of satellite overpasses can also be a contributing factor. In the morning, we might anticipate a more pronounced "cool island" effect in densely urban areas, whereas in the afternoon, we might expect a more intense "heat island" effect in those areas. Despite the inconsistent findings of previous studies, our investigation into the relationship between building height and LST across different LCZs in Sydney revealed a negative correlation between the two. We found that the effect of building height on LST is strongest during summer and spring, with correlations ranging from almost -0.2 to -0.5. This stronger negative correlation could be attributed to higher buildings providing more shading, particularly in areas with more vegetation on warm days. In contrast, during late autumn and most winter days, no significant effect is observed, particularly when combining all the LCZs. It is worth noting that there may be some misclassification in the LCZ scheme. This can be observed in Fig. 8, where some data points with building heights higher than 10m appear in compact, open, and large low-rise LCZs where building heights should range from 3-10m (Stewart and Oke, 2012).

The cooling effect of trees is noticeable especially during summer and spring, with correlations ranging from -0.2 to -0.85. It is worth noting that satellite measurements might not fully capture all shaded areas. Specifically, when shade is cast by tree crowns, these crowns can obscure a portion of the shaded region from satellite detection (depending on the solar zenith angle). The effect of low vegetation on LST is much less pronounced in most LCZs. While low vegetation is negatively correlated with LST in large low-rise areas, it shows a positive correlation in sparsely built LCZ. This disparity indicates the complexity of the impact of low vegetation on LST. For instance, recent research has shown that shaded and sun-exposed grass have distinct impacts on LST. Shaded grass can have a cooling effect, whereas grass and low vegetation exposed to direct solar radiation are not as effective at cooling surface temperature (Park et al., 2021). The variation in the impact of low vegetation on surface temperature can also be attributed to the different types of grass present in urban areas, such as dry, watered, sparse, or dense grass. A study by Wetherley et al., (2018) found a relationship between increased irrigation and decreased LST values, indicating that moisture content significantly influences the temperature-modulating effects of low vegetation.

The effect of water fraction on LST shows a clear seasonal pattern, with the strongest effect observed during summer and spring, followed by autumn, especially in compact low-rise (ranging from -0.3 to -0.5) and large low-rise areas (ranging from -0.4 to -0.6), and the weakest impact in winter.

Specifically, the weakest relationship can be seen in sparsely built areas, followed by dense tree LCZ. A study conducted in Changchun, China revealed that water significantly impacts surface temperature from autumn to spring, although this effect was not observed during winter (Yang et al., 2020). Although the water fraction in urban areas may not be a significant determinant of LST in winter, the distance from the ocean should not be overlooked. As observed in Fig. 5, distance from the coast plays an important role in shaping the local temperature distribution in winter and should be considered in urban planning and climate adaptation strategies. It is worth noting that the second selected day in summer shows a very different pattern from other summer days, although it matches summer days in terms of the range of LST and T_a (as shown in Fig. 3). This difference may be due to the fact that the day falls in March, which is typically in autumn instead of summer. These results suggest that building variables (such as building and road path fraction, frontal density, sky view factor and building height) are important factors contributing to LST variability, especially during the warmer months when there is more direct and intense solar radiation

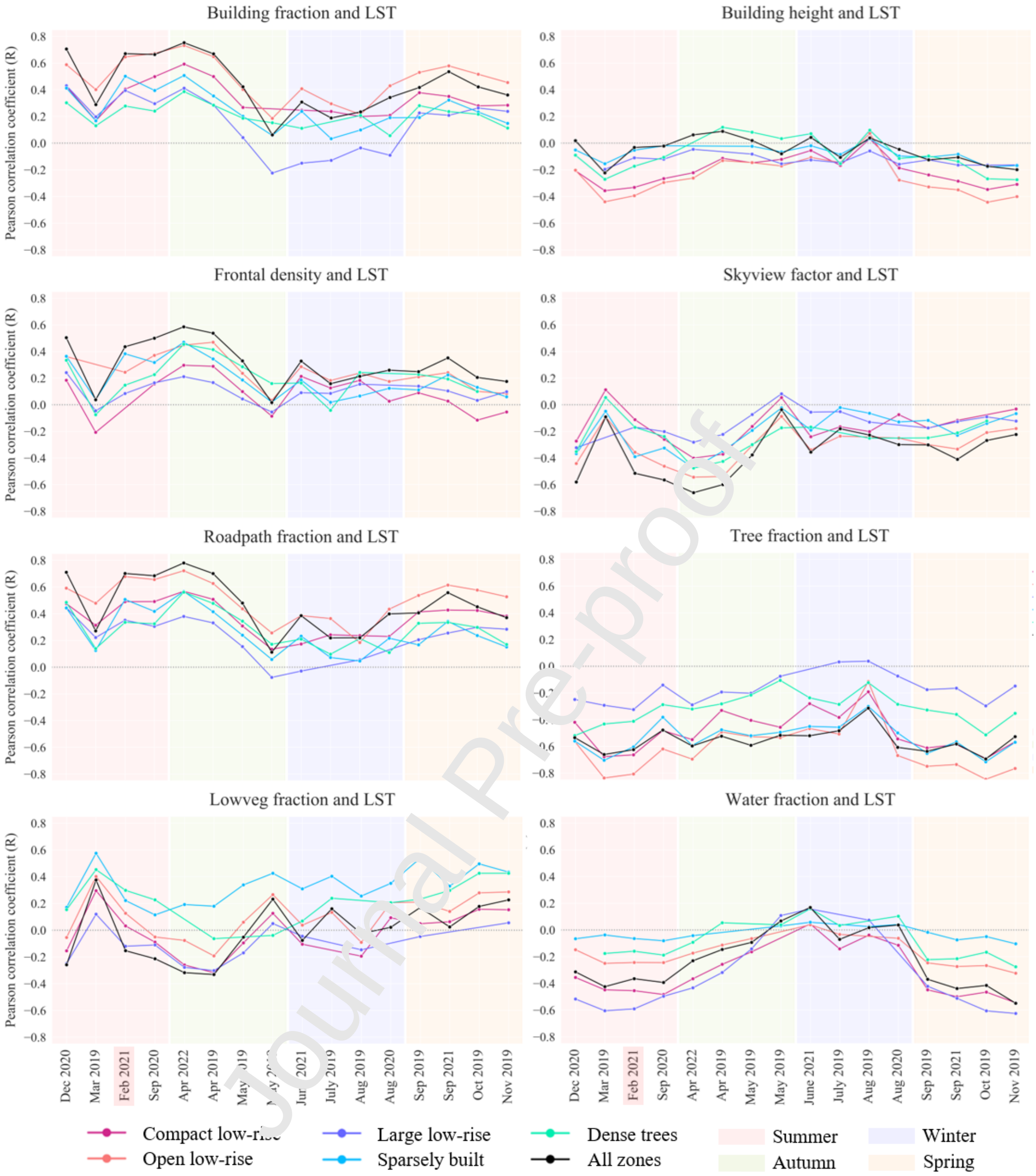

Fig. 9. The strength and direction of the correlations between Geoscape variables and LST, classified by LCZ on acquisition dates. The highlighted x-axis label (Feb 2021) corresponds to the specific summer day shown in Fig. 8, where scatterplots illustrating the correlations between Geoscape variables and LST are presented.

Due to the limited data available for T_a in all selected LCZs, even when considering crowdsourced data, most of the correlations extracted for assessing the effects of urban form and fabric on T_a are not statistically significant. Therefore, all the data was integrated into one plot (Appendix A, Fig. A. 1) to compare different LCZs across different days. In contrast to LST, there is no significant seasonal variability for the correlations between land cover variables and T_a. As shown in Fig. A. 1 in Appendix A, the strongest effect of urban form and fabric on T_a can be observed in sparsely built and large low-rise LCZs. Similar to LST, T_a was found to have positive correlations with building fraction, frontal density, and road path fraction, while showing negative correlations with tree fraction and sky view factor on most days. This shows the warming impact of building and road density on the atmosphere, while the cooling effect of open spaces and trees, respectively. Low vegetation can have a warming effect in open low-rise, but a cooling effect in compact low-rise and when combining all LCZs. This may be explained by the fact that in open low-rise areas, a significant portion of the surface is covered by impervious materials, such as concrete and asphalt, which low vegetation, like grass, cannot effectively compensate for. Moreover, the surface is not shaded in this LCZ. In contrast, in compact low-rise, shading covers a larger percentage of the area, which enhances the cooling effect of low vegetation. This increased coverage can explain why we observe a cooling effect in compact low-rise areas.

3.2.4. Explanatory power of building morphology on LST and the contributing factors

Given the uncertainty of investigating the input variables individually, we examined the combination of these urban form parameters (built-up, vegetation, and water fractions) along with terrain variables (distance from the coast and elevation) to explain the LST variation across Sydney. By analysing the combined effects of these parameters, we aim to gain a more comprehensive understanding of the complex relationships between urban morphology and surface temperature patterns in Sydney. Overall, the GB regression model used for the analysis confirmed that the variables integrated in this study could collectively well explain the variance in LST across different days in Sydney (Fig. 10).

The adjusted R^2 shows the highest values during summer (ranging from 0.78 to 0.84) and spring days (0.7 - 0.82), indicating that approximately 80% of the variation in LST can be explained by the input variables in the model. This is a strong indication that the model is a good fit for the data and that the urban morphology variables are strong predictors of LST during summer and spring. However, during winter days, the adjusted R^2 ranges from 0.44 to 0.57, which is considerably lower than that observed in summer and spring. Although the model still explains a significant amount of the variation in LST in winter days, it suggests that the urban morphology variables may not be as effective in predicting LST during cold days as they are in summer. While the adjusted R^2 shows higher values during summer and spring, the prediction error (RMSE) is the lowest during winter (0.91 - 1.33 °C) and autumn (1.02 – 1.25 °C). This suggests that there may be more uncertainty in LST prediction during warm days than in cold periods. Moreover, the RMSE value here is influenced by the distribution of temperature data. In Sydney, LST values show a wider range during summer and spring compared to autumn and winter (Fig. 3), which results in higher RMSE values in warm seasons. The dependency of RMSE on the spatial range of temperature was also observed in previous research (Venter et al., 2020), mapping T_a using remote sensing and Netatmo data. These statistics underscore the importance of accounting for seasonal variability in studies that examine the contributing factors to urban temperature characteristics.

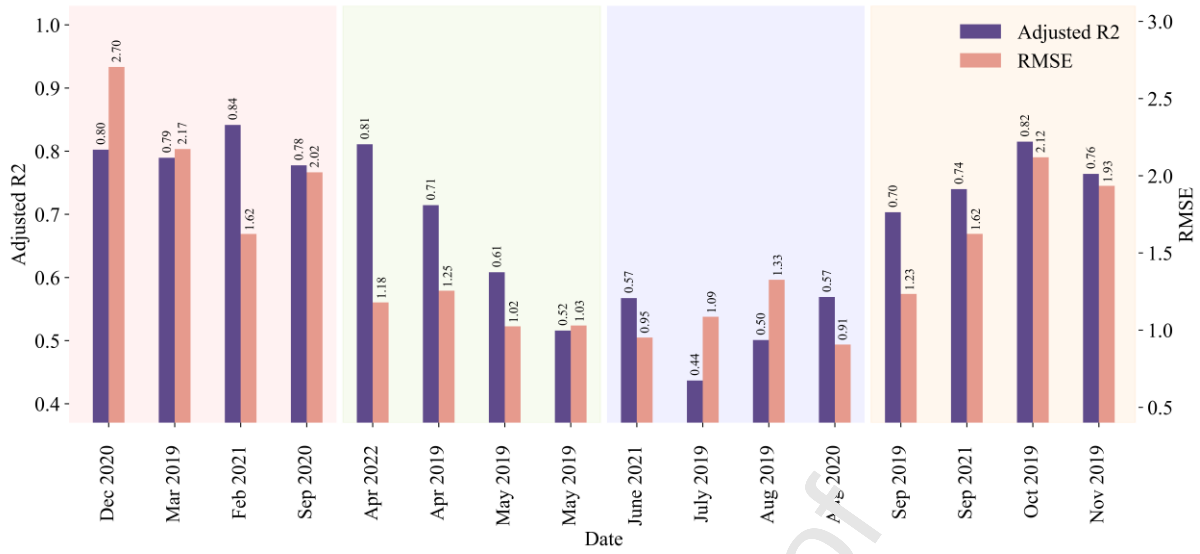

Fig. 10. Gradient boosting model performance, measured by adjusted R2 and RMSE. A comparison of explanatory potential of all variables on LST across different days and seasons (summer, autumn, winter, and spring, respectively).

To gain a better understanding of which variables have the greatest impact on explaining the variance in LST, we employed the GB model to determine the importance of features. As shown in Fig. 11, a significant seasonal variation can be observed in the dominant explanatory factors of LST in Sydney. In almost all days from December to April (summer and relatively warm days in autumn), total built, road path fraction, and building fraction have the largest contribution relative to the other factors in LST variation. However, their contribution decreases after April, with the start of the colder months, and the dominant explanatory factors change to tree fraction, followed by distance from the coast and elevation. Starting from August (the last month of winter), the moderating influence of the ocean becomes less pronounced, whereas the effect of water fraction becomes increasingly influential in explaining LST variability during spring.

A significant effect of tree fraction was observed in summer but not in winter when considering individual variables and their correlations with LST (as shown in Fig. 9). However, the opposite pattern emerges when all the variables are integrated, as observed in Fig. 11, which uses a machine learning approach to assess the importance of variables. In this integrated analysis, tree fraction shows limited predictive power for LST in summer days but becomes significant in winter (and relatively colder days in autumn and spring). Therefore, it is important to consider the combined effect of multiple variables when exploring LST variation rather than focusing solely on individual factors. Although many studies have reported the cooling effect of total vegetation cover (Estoque et al., 2017; Shiflett et al., 2017; Zhang et al., 2021), the impact of low vegetation versus tree fraction has not been explored sufficiently. While the effect of tree fraction is noticeable, particularly on cold days, low vegetation does not appear to play a significant role in LST variation. This finding highlights the complexity of the interactions between urban landscape and LST and provides valuable insights for advancing our understanding and predicting LST dynamics across different seasons.

Similar to the results shown in Fig. 9, the importance scores in the second selected day in summer show a different pattern compared to other summer days. Although this day falls within the same range of LST and T_a as other summer days (as shown in Fig. 3) and shows a similar temperature difference between LST and T_a (Fig. 4), as well as a comparable pattern of correlation between LST and T_a shown in the scatterplot (Fig. 7), the feature importance scores for this day more closely resembles that of spring days. This discrepancy may be due to the radiation levels on that day. While it is a warm day, it is not a typical summer day in terms of radiation, despite the similarities in temperature and correlation patterns.

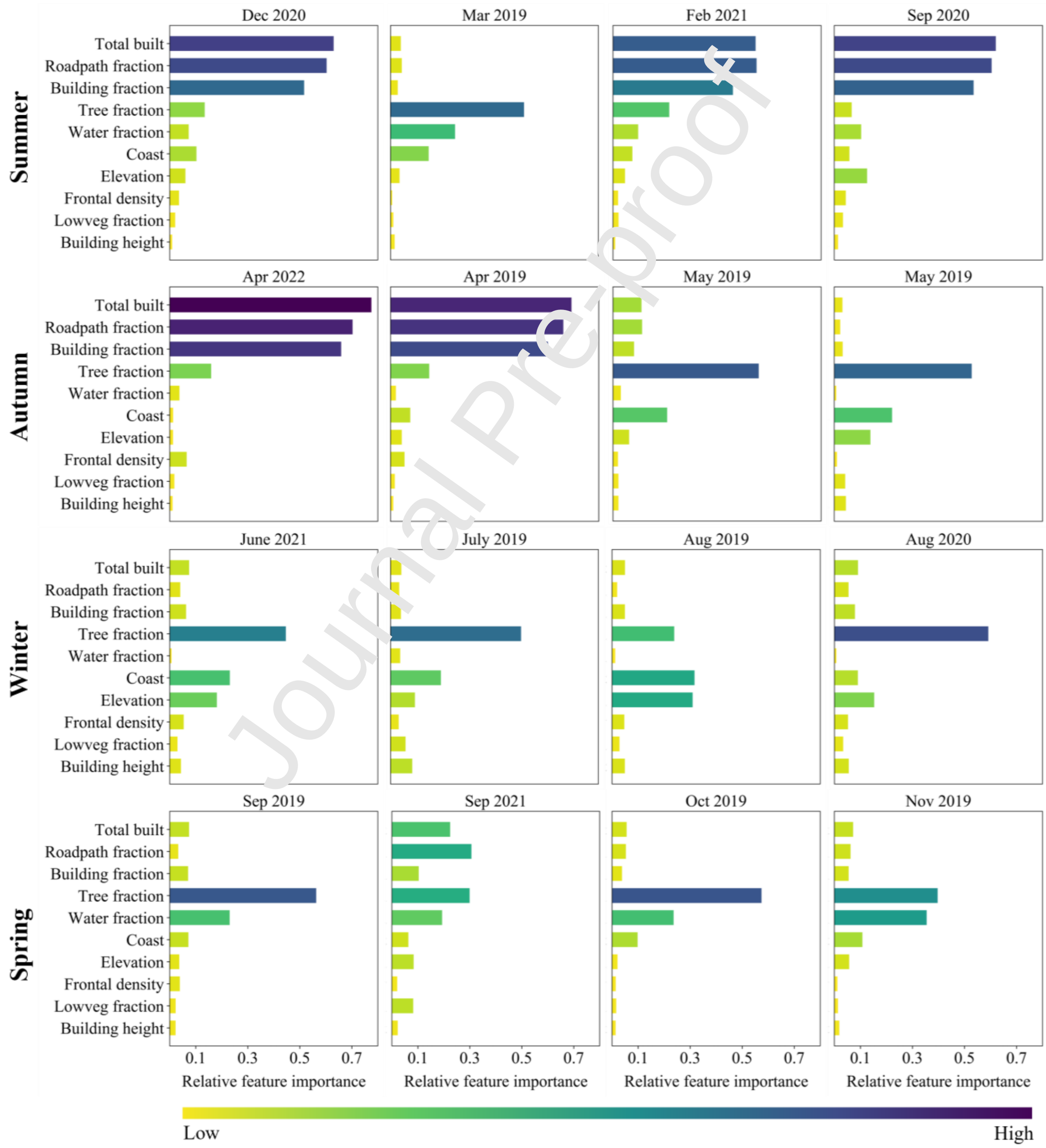

Fig. 11. Importance scores of predictor variables obtained from a trained GB model explaining LST variations across different days and seasons.

4. Conclusion

In this study, we used crowdsourced data combined with remote sensing satellite imagery (Landsat 8) to explore intra-urban and seasonal variabilities in air and surface temperature in a city with complex regional geographical influences and varied urban form. We also assessed the overlay of these datasets with building-level urban data and the LCZ scheme in order to identify the factors contributing to these variabilities. The outcomes of this study indicated that surface and air temperature have distinct characteristics, and their interaction differs by season and LCZ.

Our finding revealed that there is a greater seasonal variability in LST compared to T_a at morning overpass time. The temperature difference between LST and T_a varied depending on the season, distance from the ocean and surface cover. These factors also play significant roles in the spatial distribution of hot and cold spots for LST and T_a, particularly for LST. We observed that the distribution for T_a hot and cold spots differed from that of LST, and their respective cluster areas did not always overlap spatially. We also found that the temperature difference between LST and T_a was more pronounced in the built LCZs compared to the natural LCZs (dense and scattered trees). These findings show that LST may not fully capture the spatial variations of air temperature in urban environments.

Results from our study also indicate that urban form and seasonality modulate the relationship between LST and T_a. Classifying the measurement sites based on the LCZs they are situated within resulted in stronger correlations between LST and T_a. Natural LCZs showed stronger relationships compared to built LCZs and among the built LCZs, less densely built-up areas tended to show stronger relationships. While the relevance of this correlation is more important during summer months and in densely populated regions, it appears that the correlation is not as reliable for more dense built-up areas and during warm seasons.

Analysis of the correlation between LST and urban morphology variables revealed seasonal and intra-seasonal variations. In general, stronger relationships were observed in the summer, early and mid-autumn, and spring, while weaker relationships were observed in winter. Investigating the bivariate association between LST and land cover variables showed that trees could have a notable cooling effect, particularly during the summer and spring. However, low vegetation does not appear to play a significant role in LST variation in most LCZs. In contrast to LST, there is no significant seasonal variability for the correlations between Geoscape variables and T_a.

When investigating the impact of individual land cover variables on LST, we found that tree fraction had a significant effect during summer, but not in winter. However, when all variables were taken into account using machine learning, tree fraction was found to contribute significantly to LST variation in winter, as well as on relatively colder days in autumn and spring. This highlights the importance of considering the combined effect of multiple variables when exploring LST variability, rather than focusing solely on individual factors.

The detailed spatial information presented by this study provides insights into understanding the mechanisms of surface and air temperature variability in urban environments, including the relationship between the two and the driving factors across different seasons. We expect that the comprehensive spatial analysis presented here can further serve as a theoretical foundation for evaluating urban heat and accurately predicting air temperature based on satellite LST, which can help the development of effective heat mitigation strategies and improve thermal comfort in cities.

Despite these significant findings, there are some limitations in this study that need to be mentioned. The analysis in this study was limited to clear sky daytime data, as the Landsat satellite only provides information on daytime surface temperature. The timing of satellite overpass at 10 am might yield different heat island dynamics compared to an afternoon or evening overpass. Thus, further investigation is needed to explore diurnal variability and assess how the urban temperature dynamic may vary throughout the day. A detailed temporal analysis could also provide more insights into the relationship between surface and air temperature, especially when analysed under varying weather conditions. For a more comprehensive understanding of the complex interaction between LST and T_a, additional meteorological variables such as wind speed and humidity should also be considered. Future studies could aim to test hypotheses that focus on how differing synoptic conditions modulate the observed variations in surface and air temperatures.

Despite the higher spatial resolution of crowdsourced air temperature data, not all regions and LCZs are equally represented; open low-rise and compact low-rise have a significantly higher number of stations compared to other LCZs. Therefore, when using data like this, we recommend supplementing the analysis with additional sensors in those LCZs to ensure equitable representation of the entire population.

CRediT authorship contribution statement

Marzie Naserikia: Conceptualization, Methodology, Investigation, Software, Formal analysis, Data curation, Writing - original draft, Visualization. **Melissa A. Hart** and **Negin Nazarian:** Conceptualization, Methodology, Formal analysis, Writing – review & editing, Supervision. **Benjamin Bechtel:** Data curation, Writing – review & editing. **Mathew Lipson** and **Kerry A. Nice:** Writing – review & editing.

Data availability

The analysed dataset is available from the corresponding author on reasonable request.

Declaration of competing interest

The authors declare no competing interests.

Acknowledgements

This work was supported by the Australian Research Council as part of the Centre of Excellence for Climate Extremes (CE170100023). We would also like to acknowledge Peter Steinle and Vinod Kumar from the Australian Bureau of Meteorology for their valuable insights and constructive comments, which greatly contributed to the improvement of this manuscript.

Appendix A

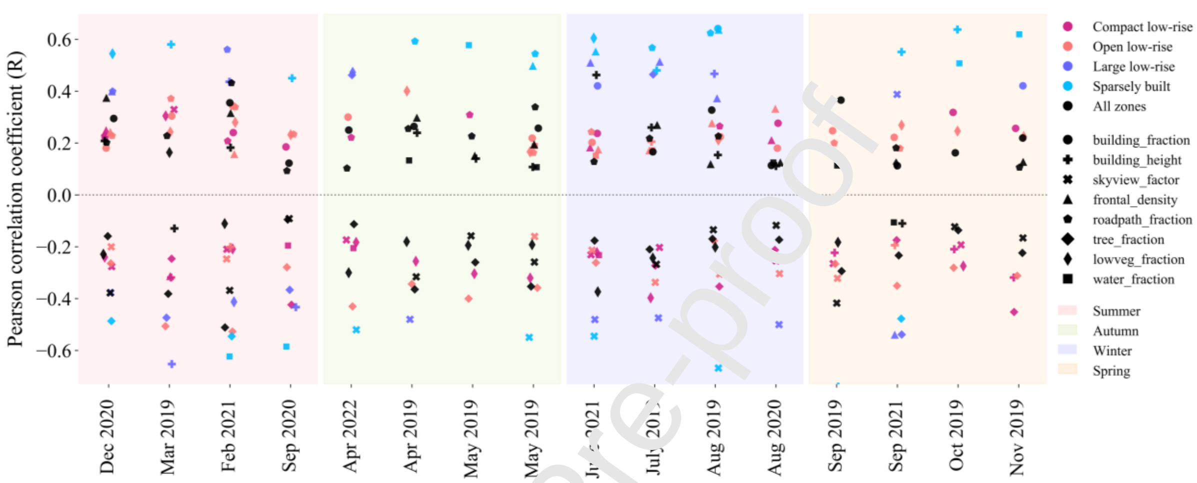

Fig. A. 1. The strength and direction of the correlations between Geoscape variables and Ta in Sydney, classified by LCZ on acquisition dates.

References

Aflaki, A., Mirnezhad, M., Ghaffarianhoseini, A., Ghaffarianhoseini, A., Omrany, H., Wang, Z.-H., Akbari, H., 2017. Urban heat island mitigation strategies: A state-of-the-art review on Kuala Lumpur, Singapore and Hong Kong. Cities 62, 131–145. https://doi.org/10.1016/j.cities.2016.09.003.

Baranka, G., Bozó, L., Komac, B., 2016. Urban Heat Island Gold Standard and Urban Heat Island Atlas, in: Counteracting Urban Heat Island Effects in a Global Climate Change Scenario. Springer, pp. 41–70. http://dx.doi.org/10.1007/978-3-319-10425-6_15.

Benali, A., Carvalho, A.C., Nunes, J.P., Carvalhais, N., Santos, A., 2012. Estimating air surface temperature in Portugal using MODIS LST data. Remote Sens. Environ. 124, 108–121. https://doi.org/10.1016/j.rse.2012.04.02.

Burnett, M., Chen, D., 2021. The impact of seasonality and land cover on the consistency of relationship between air temperature and LST derived from Landsat 7 and MODIS at a local scale: A case study in Southern Ontario. Land (Basel) 10, 672. https://doi.org/10.3390/land10070672.

Cai, M., Ren, C., Xu, Y., Lau, K.K.-L., Wang, R., 2018. Investigating the relationship between local climate zone and land surface temperature using an improved WUDAPT methodology–A case study of Yangtze River Delta, China. Urban Climate 24, 485–502. https://doi.org/10.1016/j.uclim.2017.05.010.

Cao, J., Zhou, W., Zheng, Z., Ren, T., Wang, W., 2021. Within-city spatial and temporal heterogeneity of air temperature and its relationship with land surface temperature. Landsc. Urban Plan. 206, 103979. https://doi.org/10.1016/j.landurbplan.2020.103979.

Chakraborty, T., Sarangi, C., Tripathi, S.N., 2017. Understanding Diurnality and Inter-Seasonality of a Sub-tropical Urban Heat Island. Bound.-Layer Meteorol. 163, 287–309. https://doi.org/10.1007/s10546-016-0223-0.

Chapman, L., Bell, C., Bell, S., 2017. Can the crowdsourcing data paradigm take atmospheric science to a new level? A case study of the urban heat island of London quantified using Netatmo weather stations. Int. J. Climatol. 37, 3597–3605. https://doi.org/10.1002/joc.4940.

Demuzere, M., Kittner, J., Martilli, A., Mills, G., Moede, C., Stewart, I.D., van Vliet, J., Bechtel, B., 2022. A global map of Local Climate Zones to support earth system modelling and urban scale environmental science. Earth System Science Data Discussions 2022, 1–57. https://doi.org/10.5194/essd-14-3835-2022.

Dormann, C.F., Elith, J., Bacher, S., Buchmann, C., Carl, G., Carré, G., Marquéz, J.R.G., Gruber, B., Lafourcade, B., Leitão, P.J., 2013. Collinearity: a review of methods to deal with it and a simulation study evaluating their performance. Ecography 36, 27–46. https://doi.org/10.1111/j.1600-0587.2012.07348.x.

Dousset, B., 1989. AVHRR-derived cloudiness and surface temperature patterns over the Los Angeles area and their relationship to land use. Proceedings of IGARSS-89. IEEE New York, NY, pp. 2132–2137.

Du, H., Zhan, W., Voogt, J., Bechtel, B., Chakraborty, T.C., Liu, Z., Hu, L., Wang, Z., Li, J., Fu, P., Liao, W., Luo, M., Li, L., Wang, S., Huang, F., Miao, S., 2023. Contrasting trends and drivers of global surface and canopy urban heat islands. Geophys. Res. Lett. 50. https://doi.org/10.1029/2023GL104661.

Duguay-Tetzlaff, A., Bento, V.A., Göttsche, F.M., Stöckli, R., Martins, J., Trigo, I., Olesen, F., Bojanowski, J.S., Da Camara, C., Kunz, H., 2015. Meteosat land surface temperature climate data record: Achievable accuracy and potential uncertainties. Remote Sensing 7, 13139–13156. https://doi.org/10.3390/rs71013139.

Ermida, S. L., Soares, P., Mantas, V., Göttsche, F.-M. & Trigo, I. F. 2020. Google earth engine open-source code for land surface temperature estimation from the Landsat series. Remote Sensing, 12, 1471. https://doi.org/10.3390/rs12091471.

Estoque, R.C., Murayama, Y., Myint, S.W., 2017. Effects of landscape composition and pattern on land surface temperature: An urban heat island study in the megacities of Southeast Asia. Sci. Total Environ. 577, 349–359. https://doi.org/10.1016/j.scitotenv.2016.10.195.

Fenner, D., Bechtel, B., Demuzere, M., Kittner, J., Meier, F., 2021. CrowdQC+—A Quality-Control for Crowdsourced Air-Temperature Observations Enabling World-Wide Urban Climate Applications. Front. Environ. Sci. Eng. China 9. https://doi.org/10.3389/fenvs.2021.720747. https://doi.org/10.3389/fenvs.2020.581591.

Fenner, D., Meier, F., Bechtel, B., Otto, M., Scherer, D., 2017. Intra and inter "local climate zone" variability of air temperature as observed by crowdsourced citizen weather stations in Berlin, Germany. Meteorol. Z. 26, 525–547. https://doi.org/10.1127/metz/2017/0861.

Friedman, J.H., 2001. Greedy function approximation: a gradient boosting machine. Ann. Stat. 1189–1232.

Getis, A., Ord, J.K., 2010. The analysis of spatial association by use of distance statistics. Geogr. Anal. 24, 189–206. https://www.jstor.org/stable/2699986.

Gorelick, N., Hancher, M., Dixon, M., Ilyushchenko, S., Thau, D., Moore, R., 2017. Google Earth Engine: Planetary-scale geospatial analysis for everyone. Remote Sens. Environ. 202, 18–27. https://doi.org/10.1016/j.rse.2017.06.031.

Gosling, S.N., Lowe, J.A., McGregor, G.R., Pelling, M., Malamud, B.D., 2009. Associations between elevated atmospheric temperature and human mortality: a critical review of the literature. Clim. Change 92, 299–341. https://doi.org/10.1007/s10584-008-9441-x.

Guo, G., Zhou, X., Wu, Z., Xiao, R., Chen, Y., 2016. Characterizing the impact of urban morphology heterogeneity on land surface temperature in Guangzhou, China. Environmental Modelling & Software 84, 427–439. https://doi.org/10.1016/j.envsoft.2016.06.021.

Hirsch, A.L., Evans, J.P., Thomas, C., Conroy, B., Hart, M.A., Lipson, M., Ertler, W., 2021. Resolving the influence of local flows on urban heat amplification during heatwaves. Environ. Res. Lett. 16, 064066. https://doi.org/10.1088/1748-9326/ac0377.

Ho, H.C., Knudby, A., Sirovyak, P., Xu, Y., Hodul, M., Henderson, S.B., 2014. Mapping maximum urban air temperature on hot summer days. Remote Sens. Environ. 154, 38–45. https://doi.org/10.1016/j.rse.2014.08.012.

Ho, H.C., Knudby, A., Xu, Y., Hodul, M., Aminipouri, M., 2016. A comparison of urban heat islands mapped using skin temperature, air temperature, and apparent temperature (Humidex), for the greater Vancouver area. Sci. Total Environ. 544, 929–938. https://doi.org/10.1016/j.scitotenv.2015.12.021.

Hu, Y., Hou, M., Jia, G., Zhao, C., Zhen, X., Xu, Y., 2019. Comparison of surface and canopy urban heat islands within megacities of eastern China. ISPRS J. Photogramm. Remote Sens. 156, 160–168. https://doi.org/10.1016/j.isprsjprs.2019.08.012.

Jamei, E., Rajagopalan, P., Seyedmahmoudian, M., Jamei, Y., 2016. Review on the impact of urban geometry and pedestrian level greening on outdoor thermal comfort. Renewable Sustainable Energy Rev. 54, 1002–1017. https://doi.org/10.1016/j.rser.2015.10.104.

Jin, M., Dickinson, R.E., 2010. Land surface skin temperature climatology: benefitting from the strengths of satellite observations. Environ. Res. Lett. 5, 044004. https://doi.org/10.1088/1748-9326/5/4/044004

Johansson, E., Emmanuel, R., 2006. The influence of urban design on outdoor thermal comfort in the hot, humid city of Colombo, Sri Lanka. Int. J. Biometeorol. 51, 119–133. https://doi.org/10.1007/s00484-006-0047-6.

Kim, J., Lee, D.-K., Brown, R.D., Kim, S., Kim, J.-H., Sung, S., 2022. The effect of extremely low sky view factor on land surface temperatures in urban residential areas. Sustainable Cities and Society 80, 103799. https://doi.org/10.1016/j.scs.2022.103799.

Kim, M., Wang, L., Zhou, Y., 2021. Spatially Varying Coefficient Models with Sign Preservation of the Coefficient Functions. J. Agric. Biol. Environ. Stat. 26, 367–386. https://doi.org/10.1007/s13253-021-00443-5.

Kloog, I., Nordio, F., Coull, B.A., Schwartz, J., 2014. Predicting spatiotemporal mean air temperature using MODIS satellite surface temperature measurements across the Northeastern USA. Remote Sens. Environ. 150, 132–139. https://doi.org/10.1016/j.rse.2014.04.024.

Krayenhoff, E.S., Broadbent, A.M., Zhao, L., Georgescu, M., Middel, A., Voogt, J.A., Martilli, A., Sailor, D.J., Erell, E., 2021. Cooling hot cities: A systematic and critical review of the numerical modelling literature. Environ. Res. Lett. 16, 053007. https://doi.org/10.1088/1748-9326/abdcf1.

Krelaus, L., Apfel, J., Bechtel, B., Sismanidis, P., 2023. Surface and canopy-layer urban heat island intensities in Europe – Quantifying differences in the diurnal cycle for three summer periods, in: 2023 Joint Urban Remote Sensing Event (JURSE). Presented at the 2023 Joint Urban Remote Sensing Event (JURSE), IEEE, pp. 1–4. https://doi.org/10.1109/JURSE57346.2023.10144174.

Lipson, M.J., Nazarian, N., Hart, M.A., Nice, K.A., 2022. A transformation in city-descriptive input data for urban climate models. Frontiers in Environmental Science, 10, p.866398. https://doi.org/10.3389/fenvs.2022.866398.

Liu, W., Zhang, G., Jiang, Y., Wang, J., 2021. Effective Range and Driving Factors of the Urban Ventilation Corridor Effect on Urban Thermal Comfort at Unified Scale with Multisource Data. Remote Sensing 13, 1783. https://doi.org/10.3390/rs13091783.

Livada, I., Synnefa, A., Haddad, S., Paolini, R., Garshasbi, S., Ulpiani, G., Fiorito, F., Vassilakopoulou, K., Osmond, P., Santamouris, M., 2019. Time series analysis of ambient air-temperature during the period 1970–2016 over Sydney, Australia. Sci. Total Environ. 648, 1627–1638. https://doi.org/10.1016/j.scitotenv.2018.08.144.

Ma, Q., Wu, J., He, C., 2016. A hierarchical analysis of the relationship between urban impervious surfaces and land surface temperatures: spatial scale dependence, temporal variations, and bioclimatic modulation. Landsc. Ecol. 31, 1139–1153. https://doi.org/10.1007/s10980-016-0356-z.

Martilli, A., Roth, M., Chow, W.T.L., 2020. Summer average urban-rural surface temperature differences do not indicate the need for urban heat reduction. Research Collection School of Social Sciences 1. https://doi.org/10.1038/s41586-019-1512-9.

Ma, S., Pitman, A., Hart, M., Evans, J.P., Haghdadi, N., MacGill, I., 2017. The impact of an urban canopy and anthropogenic heat fluxes on Sydney's climate. Int. J. Climatol. 37, 255–270. https://doi.org/10.1002/joc.5001.

Masson, V., Lemonsu, A., Hidalgo, J., Voogt, J., 2020. Urban Climates and Climate Change. Annu. Rev. Environ. Resour. 45, 411–444. https://doi.org/10.1146/annurev-environ-012320-083623.

Méndez-Lázaro, P., Muller-Karger, F.E., Otis, D., McCarthy, M.J., Rodríguez, E., 2018. A heat vulnerability index to improve urban public health management in San Juan, Puerto Rico. Int. J. Biometeorol. 62, 709–722. https://doi.org/10.1007/s00484-017-1319-z.

Middel, A., Nazarian, N., Demuzere, M., Bechtel, B., 2022. Urban Climate Informatics: An Emerging Research Field. Front. Environ. Sci. Eng. China 10. https://doi.org/10.3389/fenvs.2022.867434. https://doi.org/10.3389/fenvs.2022.867434.

Mou, B., He, B.-J., Zhao, D.-X., Chau, K.-W., 2017. Numerical simulation of the effects of building dimensional variation on wind pressure distribution. Engineering Applications of Computational Fluid Mechanics 11, 293–309. https://doi.org/10.1080/19942060.2017.1281845.

Mutiibwa, D., Strachan, S., Albright, T., 2015. Land surface temperature and surface air temperature in complex terrain. IEEE Journal of Selected Topics in Applied Earth Observations and Remote Sensing

8, 4762–4774. https://doi.org/10.1109/JSTARS.2015.2468594.
Naserikia, M., Hart, M.A., Nazarian, N., Bechtel, B., 2022. Background climate modulates the impact of land cover on urban surface temperature. Sci. Rep. 12, 15433. https://doi.org/10.1038/s41598-022-19431-x.
Nazarian, N., Krayenhoff, E.S., Bechtel, B., Hondula, D.M., Paolini, R., Vanos, J., Cheung, T., Chow, W.T.L., de Dear, R., Jay, O., Lee, J.K.W., Martilli, A., Middel, A., Norford, L.K., Sadeghi, M., Schiavon, S., Santamouris, M., 2022. Integrated assessment of urban overheating impacts on human life. Earths Future 10. https://doi.org/10.1029/2022EF002682.
Nice, K.A., Nazarian, N., Lipson, M.J., Hart, M.A., Seneviratne, S., Thompson, J., Naserikia, M., Godic, B., Stevenson, M., 2022. Isolating the impacts of urban form and fabric from geography on urban heat and human thermal comfort. Build. Environ. 224, 109502. https://doi.org/10.1016/j.buildenv.2022.109502.
O'Malley, C., Piroozfar, P., Farr, E.R.P., Pomponi, F., 2015. Urban Heat Island (UHI) mitigating strategies: A case-based comparative analysis. Sustainable Cities and Society 19, 222–235. https://doi.org/10.1016/j.scs.2015.05.009.
Park, Y., Guldmann, J.-M., Liu, D., 2021. Impacts of tree and building shades on the urban heat island: Combining remote sensing, 3D digital city and spatial regression approaches. Comput. Environ. Urban Syst. 88, 101655. https://doi.org/10.1016/j.compenvurbsys.2021.101655.
Potgieter, J., Nazarian, N., Lipson, M.J., Hart, M.A., Ulpiani, G., Morrison, W., Benjamin, K., 2021. Combining High-Resolution Land Use Data With Crowdsourced Air Temperature to Investigate Intra-Urban Microclimate. Front. Environ. Sci. Eng. China 9. https://doi.org/10.3389/fenvs.2021.720323.
Radhi, H., Sharples, S., Assem, E., 2015. Impact of urban heat islands on the thermal comfort and cooling energy demand of artificial islands—A case study of AMWAJ Islands in Bahrain. Sustainable Cities and Society 19, 310–318. https://doi.org/10.1016/j.scs.2015.07.017.
Schlünzen, K.H., Grimmond, S., Baklanov, A., 2023. Guidance to Measuring, Modelling and Monitoring the Canopy Layer Urban Heat Island (CL-UHI). World Meteorological Origanization, Geneva, p. 103.
Sheng, Y., Liu, X., Yang, X., Xin, Q., Deng, C., Li, X., 2017. Quantifying the spatial and temporal relationship between air and land surface temperatures of different land-cover types in Southeastern China. Int. J. Remote Sens. 38, 1114–1136. https://doi.org/10.1080/01431161.2017.1280629.
Shen, H., Jiang, Y., Li, T., Cheng, Q., Zeng, C., Zhang, L., 2020. Deep learning-based air temperature mapping by fusing remote sensing, station, simulation and socioeconomic data. Remote Sens. Environ. 240, 111692. https://doi.org/10.1016/j.rse.2020.111692.
Shiflett, S.A., Liang, L.L., Crum, S.M., Feyisa, G.L., Wang, J., Jenerette, G.D., 2017. Variation in the urban vegetation, surface temperature, air temperature nexus. Sci. Total Environ. 579, 495–505. https://doi.org/10.1016/j.scitotenv.2016.11.069.
Shreevastava, A., Prasanth, S., Ramamurthy, P., Rao, P.S.C., 2021. Scale-dependent response of the urban heat island to the European heatwave of 2018. Environ. Res. Lett. 16, 104021. https://doi.org/10.1088/1748-9326/ac25bb.
Sidiqui, P., Huete, A., Devadas, R., 2016. Spatio-temporal mapping and monitoring of Urban Heat Island patterns over Sydney, Australia using MODIS and Landsat-8. Presented at the 2016 4th International Workshop on Earth Observation and Remote Sensing Applications (EORSA), IEEE. https://doi.org/10.1109/EORSA.2016.7552800.
Stewart, I.D., Krayenhoff, E.S., Voogt, J.A., Lachapelle, J.A., Allen, M.A., Broadbent, A.M., 2021. Time evolution of the surface urban heat island. Earths Future 9. https://doi.org/10.1029/2021ef002178. https://doi.org/10.1029/2021EF002178.
Stewart, I.D., Oke, T.R., 2012. Local climate zones for urban temperature studies. Bull. Am. Meteorol. Soc. 93, 1879–1900. https://doi.org/10.1175/BAMS-D-11-00019.1.
Tan, J., Zheng, Y., Tang, X., Guo, C., Li, L., Song, G., Zhen, X., Yuan, D., Kalkstein, A.J., Li, F., 2010. The urban heat island and its impact on heat waves and human health in Shanghai. Int. J. Biometeorol. 54, 75–84. https://doi.org/10.1007/s00484-009-0256-x.
Vahmani, P., Ban-Weiss, G.A., 2016. Impact of remotely sensed albedo and vegetation fraction on simulation of urban climate in WRF-urban canopy model: A case study of the urban heat island in Los Angeles. J. Geophys. Res. 121, 1511–1531. https://doi.org/10.1002/2015JD023718.
Varentsov, M.I., Konstantinov, P.I., Shartova, N.V., Samsonov, T.E., Kargashin, P.E., Varentsov, A.I., Fenner, D., Meier, F., 2020. Urban heat island of the Moscow megacity: the long-term trends and

new approaches for monitoring and research based on crowdsourcing data. IOP Conf. Ser.: Earth Environ. Sci. 606, 012063. https://doi.org/10.1088/1755-1315/606/1/012063.

Venter, Z.S., Brousse, O., Esau, I., Meier, F., 2020. Hyperlocal mapping of urban air temperature using remote sensing and crowdsourced weather data. Remote Sens. Environ. 242, 111791. https://doi.org/10.1016/j.rse.2020.111791.

Venter, Z.S., Chakraborty, T., Lee, X., 2021. Crowdsourced air temperatures contrast satellite measures of the urban heat island and its mechanisms. Science Advances 7, eabb9569. https://doi.org/10.1126/sciadv.abb9569.

Wang, K., Jiang, S., Wang, J., Zhou, C., Wang, X., Lee, X., 2017. Comparing the diurnal and seasonal variabilities of atmospheric and surface urban heat islands based on the Beijing urban meteorological network. J. Geophys. Res. D: Atmos. 122, 2131–2154. https://doi.org/10.1002/2016JD025304.

Wetherley, E.B., McFadden, J.P., Roberts, D.A., 2018. Megacity-scale analysis of urban vegetation temperatures. Remote Sens. Environ. 213, 18–33. https://doi.org/10.1016/j.rse.2018.04.051.

World Meteorological Organization (WMO), 2021. Guide to Instruments and Methods of Observation Vol. V—Quality Assurance and Management of Observing Systems.

Yang, C., Yan, F., Lei, X., Ding, X., Zheng, Y., Liu, L., Zhang, S., 2020. Investigating Seasonal Effects of Dominant Driving Factors on Urban Land Surface Temperature in a Snow-Climate City in China. Remote Sensing 12, 3006. https://doi.org/10.3390/rs12183006.

Yang, F., Qian, F., Lau, S.S.Y., 2013. Urban form and density as indicators for summertime outdoor ventilation potential: A case study on high-rise housing in Shanghai. Build. Environ. 70, 122–137. https://doi.org/10.1016/j.buildenv.2013.08.019.

Yang, J., Jin, S., Xiao, X., Jin, C., Xia, J.C., Li, X., Wang, S., 2019. Local climate zone ventilation and urban land surface temperatures: Towards a performance-based and wind-sensitive planning proposal in megacities. Sustainable Cities and Society 47, 101487. https://doi.org/10.1016/j.scs.2019.101487.

Yang, Y.Z., Cai, W.H., Yang, J., 2017. Evaluation of MODIS Land Surface Temperature Data to Estimate Near-Surface Air Temperature in Northeast China. Remote Sensing 9, 410. https://doi.org/10.3390/rs9050410.

Yun, G.Y., Ngarambe, J., Duhirwe, P.N., Ulpiani, G., Paolini, R., Haddad, S., Vasilakopoulou, K., Santamouris, M., 2020. Predicting the magnitude and the characteristics of the urban heat island in coastal cities in the proximity of desert landforms. The case of Sydney. Sci. Total Environ. 709, 136068. https://doi.org/10.1016/j.scitotenv.2019.136068.

Zhang, P., Bounoua, L., Imhoff, M.L., Wolfe, R.E., 2014. Comparison of MODIS land surface temperature and air temperature over the continental USA meteorological stations. Canadian Journal of.

Zhang, Y., Balzter, H., Li, Y., 2021. Influence of Impervious Surface Area and Fractional Vegetation Cover on Seasonal Urban Surface Heating/Cooling Rates. Remote Sensing 13, 1263. https://doi.org/10.3390/rs13071263.

Zheng, Z., Zhou, W., Yan, J., Qian, Y., Wang, J., Li, W., 2019. The higher, the cooler? Effects of building height on land surface temperatures in residential areas of Beijing. Physics and Chemistry of the Earth, Parts A/B/C 110, 149–156. https://doi.org/10.1016/j.pce.2019.01.008.

Zhou, D., Xiao, J., Bonafoni, S., Berger, C., Deilami, K., Zhou, Y., Frolking, S., Yao, R., Qiao, Z., Sobrino, J.A., 2019. Satellite remote sensing of surface urban heat islands: Progress, challenges, and perspectives. Remote Sensing 11, 48. https://doi.org/10.3390/rs11010048.

Zhou, X., Okaze, T., Ren, C., Cai, M., Ishida, Y., Watanabe, H., Mochida, A., 2020. Evaluation of urban heat islands using local climate zones and the influence of sea-land breeze. Sustainable Cities and Society 55, 102060. https://doi.org/10.1016/j.scs.2020.102060.

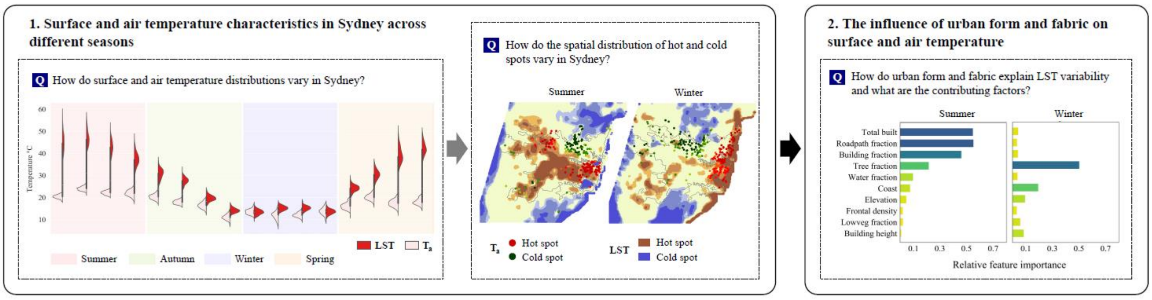

Graphical abstract

Highlights

- Urban form and seasonality modulate the relationship between LST and T_a.
- Temperature difference between LST and T_a is greater in the built LCZs compared to the natural LCZs, especially during warm days.
- Built LCZs that have less building density tend to show stronger LST-T_a relationships.
- LST does not fully capture the seasonal and spatial variability in urban thermal environments.